AD-A053 107 DEFENCE RESEARCH ESTABLISHMENT VALCARTIER (QUEBEC) F/G 14/5
DIGITAL RESTORATION OF BLURRED PHOTOGRAPHS,(U)
FEB 78 J F BOULTER
UNCLASSIFIED DREV-R-4107/78 NL

| OF |
ADA
053107

END
DATE
FILMED
6-78
DDC

UNCLASSIFIED

CRDV RAPPORT 4107/78
DOSSIER: 3633A-040
FÉVRIER 1978

DREV REPORT 4107/78
FILE: 3633A-040
FEBRUARY 1978

DIGITAL RESTORATION OF BLURRED PHOTOGRAPHS

J.F. Boulter

Centre de Recherches pour la Défense
Defence Research Establishment
Valcartier, Québec

BUREAU - RECHERCHE ET DEVELOPPEMENT
MINISTERE DE LA DÉFENSE NATIONALE
CANADA

NON CLASSIFIÉ

RESEARCH AND DEVELOPMENT BRANCH
DEPARTMENT OF NATIONAL DEFENCE
CANADA

CRDV R-4107/78
DOSSIER: 3633A-040

UNCLASSIFIED

(14) DREV-R-4107/78
FILE: 3633A-040

(3)

(6)

DIGITAL RESTORATION OF BLURRED PHOTOGRAPHS

by

(10) J. F. Boulter

(11) Feb 78

(12) 67 p.

CENTRE DE RECHERCHES POUR LA DEFENSE
DEFENCE RESEARCH ESTABLISHMENT
VALCARTIER
Tel. (418) 844-4271
Quebec, Canada

February/février 1978

NON CLASSIFIE

404 945

RESUME

La quantité d'information observable dans une photographie brouillée peut être augmentée si l'image est traitée dans un calculateur numérique. On décrit une procédure complète (qui est basée sur le filtrage de type Wiener) pour la reconstitution des photographies de haute résolution qui sont détériorées par plusieurs sortes de brouillage commun. On considère en détail les aspects pratiques d'une reconstitution acceptable. On décrit les limitations du filtre de Wiener, les caractéristiques du film photographique et des méthodes d'identification des brouillages par l'analyse des photographies brouillées. Des photographies de haute résolution défocalisées et détériorées par le mouvement qui est introduit directement dans la caméra sont reconstituées pour illustrer les techniques. (NC)

ABSTRACT

The amount of information that a human observer can obtain from a blurred photograph can be increased by post-processing the image in a digital computer. A complete procedure for restoring (by Wiener filtering) high-resolution photographs degraded by several common types of blurs is described. The practical aspects of obtaining an acceptable restoration are considered in detail. These include the limitations of the Wiener filter, the characteristics of photographic film and methods to identify the blur by analysing the blurred image using only limited a priori knowledge. High-resolution photographs degraded by motion and focus blurs introduced directly in a camera are restored to illustrate the techniques. (U)

TABLE OF CONTENTS

1.0 INTRODUCTION

Blurring of photographs can result from accidental causes (e.g. an improperly focused camera) or from more fundamental limitations (e.g. imaging through a turbulent atmosphere). In some cases the blurring cannot be eliminated a priori (i.e. the photograph cannot be taken again with the camera in focus or the object cannot be viewed through less atmosphere). The present report describes restoration of such blurred photographs by post-processing using a digital computer.

A number of approaches to the problem of digital image restoration exist. These have been reviewed by Frieden (ref. 1), Hunt (ref. 2), Andrews (ref. 3), Sondhi (ref. 4) and by Huang (ref. 5). Techniques which have successfully been used to restore medium- or high-resolution digital images include: the homomorphic restoration of Oppenheim, Stockholm and Cannon (refs. 6-9), the constrained least-squares method of Hunt (ref. 10) and Wiener filtering (refs. 11-18). Also of interest is the maximum-entropy approach of Frieden (refs. 19 and 20) and Bayesian estimation (refs. 21-23). Additional digital image restoration techniques are described in refs. 24-35 while procedures which deal specifically with restoration of blurred photographs are given in refs. 14 and 16.

Much of the current research on digital image restoration is based on the use of nonlinear rather than linear techniques. Nonlinear techniques are potentially superior to linear ones, particularly at low signal-to-noise ratio, but are more difficult to perform and require longer computing times. Most of the nonlinear methods are also

iterative. On the other hand, linear methods are more easily analysed and efficient algorithms such as the fast Fourier transform (FFT) (refs. 17, 26 and 36) can be used for certain types of linear restoration.

We describe here a procedure for restoring blurred photographs based on one of the linear techniques - Wiener filtering - implemented in the spatial-frequency domain using the FFT algorithm. Practical aspects of obtaining an acceptable restoration are emphasized. In many cases, such filtering can produce useful restorations of high-resolution photographs degraded by several common types of blurs. It can be implemented on a medium-scale digital computer or on a minicomputer with a special-purpose hardware processor.

Characteristics of photographic film, including granularity and nonlinearity, are first described and the criteria for digitizing the film are given. The Wiener filter is related to restoration of blurred photographs. Problems associated with film nonlinearity and noise, spatial variance of the blur and with edge effects are considered. Examples which demonstrate the removal of simulated out-of-focus, linear-motion and long-exposure atmospheric turbulence blurs are given. Photographs containing out-of-focus and motion blurs introduced directly in the camera are analysed to determine the nature of the blur and are restored. Two methods for determining the type of the blur (e.g. focus) and its extent (e.g. diameter of blur circle) directly from the blurred image are described.

This work was performed at DREV during 1976-77 under PCN 33A40, "Digital Image Processing".

2.0 FILM CHARACTERISTICS

2.1 Film Noise

The photographic film itself usually limits the extent to which a blurred photograph can be restored. We first consider the characteristics of photographic film which are relevant to the restoration problem.

The average density of a normal silver halide film is produced by the superposition of a number of opaque silver grains. If a film with uniform average density is digitized, the resulting density measurements will not be constant. They will fluctuate around the mean density due to random variations in the size, shape and number of silver grains included in the aperture. These random fluctuations are referred to as film noise. The fluctuations are additive in density (multiplicative in transmittance) (ref. 2) and the density fluctuations have a power spectrum which can be considered flat to the cutoff frequency of the film (refs. 37-39).

The RMS density fluctuation at average density D_o, $S_D(D_o,A_o)$ is often quoted by the film manufacturer as a measure of film granularity (usually D_o=1 and A_o is the area of a circular aperture with a diameter of 48 μm). Larger apertures average more film grains and produce a lower noise level. Provided that the aperture is much larger than the grain size (e.g. 10 times larger diameter), the density fluctuations measured using apertures with different areas A and A_o are related by the Selwyn law (refs. 40 and 41):

$$S_D(D_o,A) = S_D(D_o,A_o)\sqrt{\frac{A_o}{A}} \tag{1}$$

Film noise can also be expressed as an RMS fluctuation in transmittance around a mean transmittance T , $S_T(T,A)$. For a density well above the fog level of the film (i.e. the density corresponding to zero exposure), the density and transmittance fluctuations are related (ref. 40):

$$S_T(T,A) = \frac{T\,S_D(D,A)}{0.4343} \tag{2}$$

where $T=10^{-D}$. If the film noise (S_T) is known at one transmittance T_o, it can be calculated at another transmittance T (ref. 40):

$$S_T(T,A) = S_T(T_o,A)\sqrt{\frac{T(1-T)}{T_o(1-T_o)}} \tag{3}$$

Substituting Eqs. 1 and 2 into Eq. 3 gives expressions for the film noise (S_T and S_D) in terms of the known film noise $S_D(D_o,A_o)$ and the area A of the aperture used to digitize the film:

$$S_T(T,A) = \frac{S_D(D_o,A_o)}{0.4343}\sqrt{\frac{A_o}{A}}\sqrt{\frac{T_oT(1-T)}{1-T_o}} \tag{4}$$

$$S_D(D,A) = S_D(D_o,A_o)\sqrt{\frac{A_o}{A}}\sqrt{\frac{T_o(1-T)}{T(1-T_o)}} \tag{5}$$

where $T=10^{-D}$ and $T_o=10^{-D_o}$.

We define the signal-to-noise ratio of a digitized transmittance value T as:

$$SNR(T) = \frac{T}{T\, S_T(T,A)} = \frac{1}{S_T(T,A)} \tag{6}$$

Using Eq. 4, one can write:

$$SNR(T) = \frac{0.4343}{S_D(D_o,A_o)} \sqrt{\frac{A}{A_o}} \sqrt{\frac{1-T_o}{T_o T(1-T)}} \tag{7}$$

The signal-to-noise ratio given by Eq. 7 is plotted as a function of transmittance in Fig. 1. The scale on the left has been divided by $A^{1/2}$ (in micrometers) and has been multiplied by $S_D(D_o,A_o)$ (in density units) to give a scale which applies for arbitrary film granularity and digitizing aperture. The standard conditions D_o=1 and A_o, the area of a circular aperture with a 48-μm diameter, were assumed.

This graph allows one to estimate the signal-to-noise ratio of a film with known granularity that was digitized with a given aperture. As will be described in Sec. 3.0, a value for the signal-to-noise ratio must be specified in the filter used to restore a blurred image. Secondly, if the signal-to-noise ratio of the film is known, the maximum amount of restoration possible for a given blurred image can be estimated before the restoration is actually attempted.

As an example illustrating the use of this graph, a photograph recorded on a Panatomic-X film was digitized with a 100- μm square aperture. The RMS variances within 6 small uniformly exposed areas of the film were calculated. Using Eq. 5, we converted each RMS variance to the above standard values of D_o and A_o and we averaged the 6 values to obtain the result $S_D(D_o,A_o) = 0.020$. The left-hand scale on the graph was divided by this film granularity and multiplied by the square

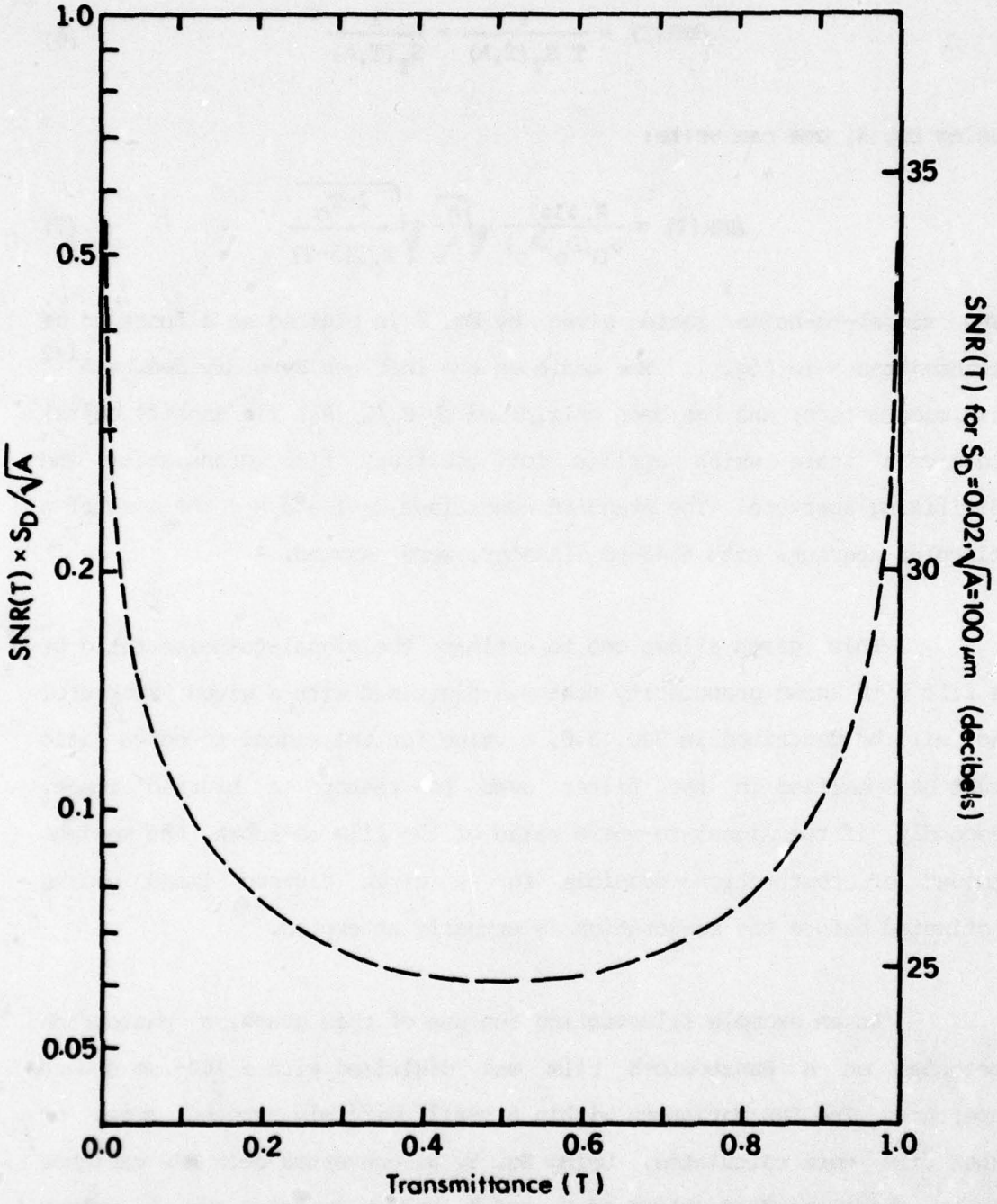

FIGURE 1 The signal-to-noise ratio of silver halide film as a function of film transmittance

root of the area of the digitizing aperture $A^{1/2}$=100 μm. The resulting signal-to-noise ratio, expressed in decibels, is shown on the right-hand scale of the graph. Note that a factor of 2 decrease in the diameter of the digitizing aperture, or a factor of 2 increase in the film granularity, decreases the signal-to-noise ratio by 3 dB at any transmittance.

The signal-to-noise ratio of the film depends significantly on the density. In the present example, regions of the film with a transmittance of 0.5 (D=0.30) have a 25-db signal-to-noise ratio while regions with low average transmittance (T=0.05, D=1.30) or with high average transmittance (T=0.95, D=0.022) have a signal-to-noise ratio increased to 29 dB. This means that (neglecting the effects of film nonlinearity), it will be more difficult to restore regions with an average transmittance near 0.5 than regions with a higher or a lower average transmittance (Sec. 3.0).

The above noise calculations are based on the probability of overlap of the developed silver grains. At low exposure levels additional noise due to variation in the number of silver grains activated by the light photons will contribute. This (along with other possible noise sources) will decrease the effective signal-to-noise ratio below that predicted by Eq. 7.

2.2 Film Transfer Function

An exposure g(x,y) will produce a film density:

$$D(x,y) = \gamma \log[g(x,y)] - D_f \qquad (8)$$

where γ is the film gamma (γ is positive for negative film and negative for positive film) and D_f is the fog level of the film. One obtains the transmittance through the film $T(x,y)$ by exponentiating the density:

$$T(x,y) = 10^{D(x,y)} = 10^{-D_f}[g(x,y)]^{\gamma} \tag{9}$$

It is evident from Eq. 9 that the film transmittance is linearly related to the original exposure only if $\gamma=1$.

In addition to a non-unity γ, a number of other effects can produce a nonlinear relationship between film exposure and transmittance. The response given by Eq. 8 does not hold for very high or very low exposure levels. Adjacency effects (ref. 42) during development tend to sharpen the boundary between two areas of different exposure. This is caused by a redistribution of developer and reaction products across the boundary which changes the rate of development. Light scattering within the film emulsion during exposure (halation) will tend to spread out a sharp boundary (ref. 42). The effect of attempting to restore a blurred image after modification by the nonlinearities present in the transfer function of the film is considered in Sec. 3.2.

2.3 Film Digitization

The first step in the present restoration procedure is to digitize the film image (convert it to digital computer format). This is performed by sampling the film image point by point using a given aperture and sampling interval (usually the aperture diameter is equal

to the sampling interval). For each point (image element), the film transmittance or density is measured and quantized into a finite number of levels. The quantization in space and density (or transmittance) must be fine enough to preserve all the information of interest in the film image and to prevent aliasing. The present section discusses criteria for performing correct spatial and density quantization.

Quantization of film density rather than film transmittance is often preferred because, in most cases, the resulting values are more uniformly distributed (ref. 29). As is evident from Eq. 3, the noise S_T is maximum at transmittance T=0.5 (D=0.30). Following Billingsley (ref. 40), we choose the size of the density steps ΔD equal to 3 times the noise S_D at this density:

$$\Delta D = 3\, S_D(D=0.3, A) \tag{10}$$

Using Eq. 5, the density step size can be written in terms of the known film noise $S_D(D_o, A_o)$ and the area of the digitizing aperture A:

$$\Delta D = 3\, S_D(D_o, A_o) \sqrt{\frac{A_o}{A}} \sqrt{\frac{T_o}{1-T_o}} \tag{11}$$

For example, using a 100 μm square aperture to digitize the Panatomic-X film described in Sec. 2.1 ($S_D(D_o, A_o) = 0.02$ where $D_o = 1$ and A_o is the area of a circular aperture with 48-μm diameter) requires a density step size $\Delta D = 0.0085$. If a 3D density range is to be digitized, then at least $3/\Delta D = 354$ uniformly spaced density levels are required.

In performing the spatial quantization, one has to assume that the film image band-limited to an upper spatial frequency W_o. The sampling interval must then be $1/2W_o$ or less to preserve the highest spatial frequency. Band-limiting of the film image can result from the spatial-frequency content of the original scene which was photographed, or it can correspond to the cutoff of the camera lens or photographic film. (For example, taking the cutoff frequency of Kodak Plus-X film to be 50 cycles/mm (ref. 42) requires a sampling interval of 10 μm or less.)

3.0 WIENER FILTER RESTORATION

3.1 Restoration Filter

Assume that a degraded image has been produced in the following manner. First, a blur defined by a spatially invariant point-spread function $h_c(x,y)$ is convolved with the "ideal" image $f_c(x,y)$. The point-spread function (PSF) is the result obtained when the blur is applied to a single point. Spatial invariance means that the blur is the same throughout the image. Random noise $n(x,y)$ with zero mean is then added to produce the degraded image $g_c(x,y)$ available for restoration:

$$g_c(x,y) = \int_{-\infty}^{\infty}\int_{-\infty}^{\infty} h_c(x',y')\ f_c(x-x',y-y')\ dx'dy' + n(x,y) \qquad (12)$$

The model assumed for the degradation is shown schematically in the upper part of Fig. 2.

Consider the discrete function $g(x,y)$ obtained by digitizing a region of the continuous image $g_c(x,y)$ over an N- by N-element matrix. Continuous spatial functions have the subscript "c" while the corresponding sampled functions have no subscript. Within a normalization factor, the 2-dimensional discrete Fourier transform of $g(x,y)$ is given by (ref. 26):

$$G(u,v) = \sum_{x=0}^{N-1}\sum_{y=0}^{N-1} g(x,y)\ \exp[-2\pi i(ux+vy)/N] \qquad (13)$$

DEGRADATION

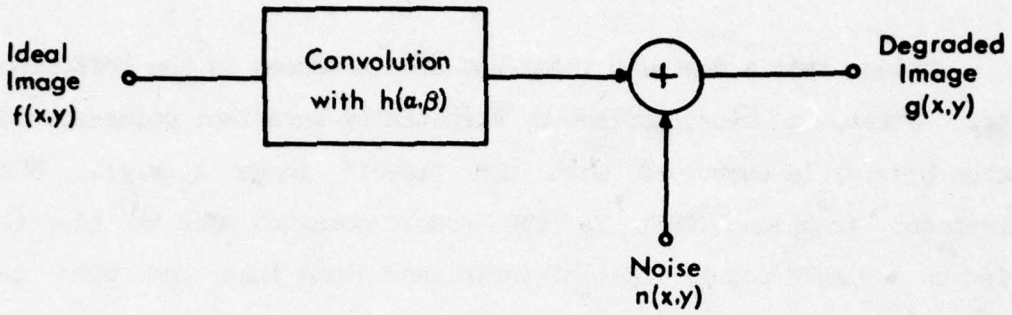

RESTORATION

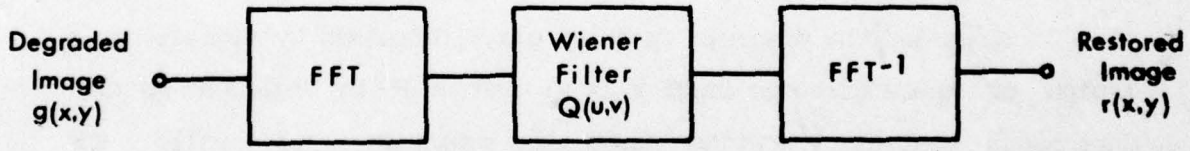

FIGURE 2 Block diagrams of the Wiener-filter restoration procedure (lower) and of the model assumed for the degraded image (upper)

and the inverse transform by:

$$g(x,y) = \sum_{x=0}^{N-1}\sum_{y=0}^{N-1} G(u,v)\ \exp[2\pi i(ux+vy)/N] \tag{14}$$

In the spatial-frequency domain, one may perform the convolution given in Eq. 12 by multiplying the discrete Fourier transform of the ideal image by the discrete Fourier transform of the PSF of the blur:

$$G(u,v) = F(u,v)\ H(u,v) + N(u,v) \tag{15}$$

The discrete Fourier transform of the PSF of the blur H(u,v) is henceforth referred to as the optical transfer function (OTF) of the blur.

The restoration problem consists in estimating f(x,y) given g(x,y). One objective criterion for performing the restoration is to minimize the mean-square error between the ideal image and the restored image r(x,y). Under the above assumptions the linear shift-invariant filter which minimizes the mean-square error has a frequency response (refs. 5 and 17):

$$Q(u,v) = \frac{H^*(u,v)}{|H(u,v)|^2 + \phi_n(u,v)/\phi_f(u,v)} \tag{16}$$

where H(u,v) is the OTF (the asterisk refers to the complex conjugate),

$\phi_n(u,v)$ is the power spectrum of the noise, and

$\phi_f(u,v)$ is the power spectrum of the ideal image.

This is generally referred to as the Wiener restoration filter (refs. 1-3) although it was first derived in the context of image restoration by Helstrom (ref. 11). Other restoration criteria have led to filters with a similar form (e.g. refs. 1-4 and 10).

The restored image $r(x,y)$ is obtained by calculating the discrete Fourier transform of $g(x,y)$ (using a 2-dimensional FFT algorithm as described in refs. 17, 45 and 47), multiplying by the Wiener filter (Eq. 16):

$$R(u,v) = G(u,v)\, Q(u,v) \tag{17}$$

and calculating the inverse discrete Fourier transform. The restoration procedure is shown schematically in the lower part of Fig. 2. Problems associated with application of this method to restore blurred photographs are discussed in Secs. 3.2, 3.3 and 3.4.

3.2 Application to Blurred Photographs

The Wiener filter given by Eq. 16 assumes that convolving a spatially invariant PSF with the ideal image and adding random noise produces the image to be restored. Most image blurs of interest are to some extent spatially variant and film noise is not additive with exposure (Sec. 2.1). Lastly, the image available for restoration is not the exposure but the exposure after modification by the nonlinear transfer function of the film (Sec. 2.2). The effect that these deviations from the assumed model can have on the restoration of blurred photographs is considered next.

Spatial invariance of the degradation means that the same PSF is convolved with all regions of the image. Some blurs are spatially invariant, others are not. For example, if all regions of the scene being photographed are located at the same range from the lens of an out-of-focus camera, then the blur will be the same throughout the image (i.e. spatially invariant). On the other hand, the images of objects located at different ranges from an out-of-focus camera will be blurred by different amounts (i.e. the blur will be spatially variant).

If, for example, an image containing spatially variant focus blur is restored by Wiener filtering using one assumed value of blur-circle diameter, only regions of the image which are blurred by approximately that amount will be correctly restored - other regions will be either over or under restored. The amount of spatial variance that can be present before the Wiener filter no longer produces an acceptable restoration depends on a number of factors. One factor is the amount of restoration sought (a large amount of restoration, which is obtained when a small value of ϕ_n/ϕ_f is specified in Eq. 16, requires a more accurate estimate for the PSF). Other factors are the type and extent of the blur (a blur with a large PSF requires that the PSF be known to a lower percent error as shown in ref. 18). Additional problems can arise when artifacts generated by incorrect restoration of one region of an image extend into correctly restored regions. Examples illustrating acceptable restorations of photographs containing blurs with both large and small amounts of spatial variance are given in Sec. 4.2.

The main source of noise in photographic imagery is usually film granularity. This noise is additive in film density and therefore multiplicative, not additive, in film transmittance (Sec. 2.1). Whether it is preferable to take the correct blurring model and restore the film transmittance image, or to take the correct noise model and restore the density image (and then exponentiate to obtain the restored transmittance image) can depend on the nature of the particular image. Neither approach is consistent with the model assumed in Eq. 16. If the image to be restored were recorded on low-granularity film, then restoration of the transmittance image could be preferable. Here the extent of the possible restoration may not be limited by film noise but rather by other effects, such as film nonlinearity or the accuracy to which the PSF can be determined (or is spatially invariant). For high-granularity film where the restoration is noise-limited, restoration of the density image could yield a better result. Density-domain restoration also has the advantage that it constrains the restored image to contain no negative values as is required for all images formed with incoherent light. Examples comparing density- and transmittance-domain restorations of blurred photographs are given in Sec. 4.2.

The Wiener filter assumes that the PSF of the blur is convolved with the original film exposure. Digitizing the film transmittance or density produces the image to be restored. A nonlinear relationship between film exposure and the image being restored (e.g. due to film nonlinearity or to restoration of the density rather than transmittance image) can adversely affect the restoration.

Such nonlinearities should have a significant effect only if they are appreciable over the area of the PSF of the Wiener filter. For example, nonlinearity due to film gamma should be important only in regions of the image where the power-law relationship between film exposure and transmittance (Eq. 9) is not approximately linear over the PSF of the Wiener filter. Similarly, restoration of the density rather than the transmittance image should be acceptable in all regions where the logarithmic density function can be considered linear over the PSF of the Wiener filter. Gradual nonlinearities where the above small-signal approximation is valid (e.g. nonlinearities due to film gamma or density-domain restoration) should be less detrimental than sharper nonlinearities (e.g. film saturation).

It must be remembered that the PSF of the Wiener restoration filter can be considerably larger than the PSF of the blur. The PSFs of the Wiener filters required to restore out-of-focus, linear-motion and long-exposure atmospheric turbulence blurs are shown, enlarged, in Fig. 3 along with the PSF of each blur. Each blur and the corresponding restoration filter are to the same scale.

3.3 Artifact Generation

The Wiener filter can introduce artificial features into the restored image which are not present in the ideal image (ref. 43). This is distinct from enhancement of noise by the filter as artifacts generally have a well-defined rather than a random structure. For example, restoration of a blurred image using the incorrect OTF in the Wiener filter (Sec. 3.2) can under some conditions generate artifacts.

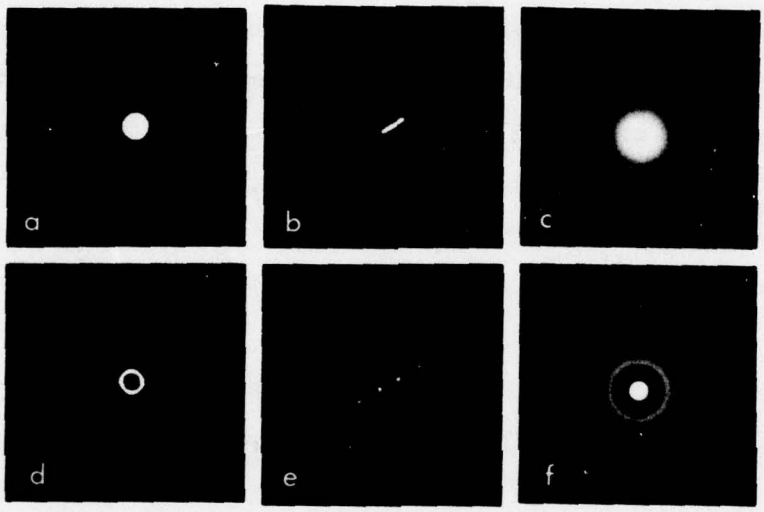

FIGURE 3 Point-spread functions of three common image blurs: (a) out-of-focus, (b) linear-motion and (c) long-exposure atmospheric transmission. The PSF s of the Wiener filters used to restore the 3 blurs are given in (d), (e) and (f) respectively.

Two other types of artifacts which are often observed in the restored image are described here.

Ringing can take place if the Wiener filter is applied to defects introduced after the blurring has occurred. Such defects could be caused, for example, by specks of dirt or scratches on the film or by sharp nonlinearities (e.g. due to film saturation). A defect with a sufficiently small area will generate an artifact consisting of a replica of the PSF of the Wiener filter. The PSFs of the Wiener filters used to restore 3 types of blur are shown, enlarged, in Fig. 3. If one of these "signatures" is observed in the restored image, it can indicate the presence of a defect in the original image. If a defect or a small-area nonlinearity can be detected by inspection of the image either before or after restoration, then the corresponding artifact can usually be reduced by appropriate editing (e.g. the affected area of the original image can be replaced if the surrounding image elements are extrapolated).

Artifacts can also be produced at the edges of the restored image. Image elements within a distance equal to the PSF of the Wiener filter from the edges of the original image cannot be correctly restored. Oscillation of the edges of the image can occur if the image borders are not properly treated before restoration. One way to minimize this artifact is to multiply the image to be restored by a window function (e.g. refs. 36 and 44) to make its edges go smoothly to zero. Another approach is to match the opposite edges of the image to one another over a given border region by fitting a low-order polynomial (ref. 15). Since the present fast Fourier transform filtering assumes

that the opposite edges of the image are adjacent (e.g. refs. 26 and 36), the latter approach was used here. In most cases, a linear interpolation over a region 5 image elements wide around the border of each 512- by 512-element image was sufficient to reduce edge effects to an acceptable level (ref. 45). This procedure was superior to the use of a bell-cosine window function (ref. 36) in its ability to reduce oscillation and also required modification of fewer image elements.

3.4 Signal-to-Noise Ratio of Wiener Filter

To optimize (in a least mean-square error sense) the restoration of a blurred image in the presence of noise, the ratio of the power spectrum of the noise to the power spectrum of the ideal image must be specified in the Wiener filter. In effect, this ratio determines the amount of restoration performed by the filter. This ratio is related to the signal-to-noise ratio of the film obtained in Sec. 2.1.

We interpret $\phi_f(u,v)$ not as the power spectrum of the ideal image but rather as a weighting factor which represents the relative importance of various spatial frequencies in the image in conveying useful information. Assume further that it is equally important to restore all spatial frequencies (up to the Nyquist frequency) independent of their actual probability of occurrence in the ideal image (i.e. $\phi_f(u,v)$=constant). Since the spatial-frequency content of many images falls off rapidly at high spatial frequencies (e.g. ref. 6), this will yield a restored image with a higher mean-square error. However, the edge or small-area structure represented by the higher spatial

frequencies is often of much interest. The assumption is that it is preferable to accept a higher mean-square error (resulting in a restored image with a noisier appearance) in order to obtain additional restoration of edge and small-area structure.

Setting $\phi_n(u,v)$ equal to the power spectrum of the film noise (which is assumed to be uniform as described in Sec. 2.1) makes the ratio $\phi_f(u,v)/\phi_n(u,v)$ constant as a function of spatial frequency. As an estimate for this ratio, we equate it to the signal-to-noise ratio of the film given by Eq. 7 at the average transmittance T_{av}:

$$\frac{\phi_f(u,v)}{\phi_n(u,v)} = \frac{0.4343}{S_d(D_o,A_o)} \sqrt{\frac{A}{A_o}} \sqrt{\frac{1-T_o}{T_o T_{av}(1-T_{av})}} \qquad (18)$$

Equation 18 gives an estimate for the amount of restoration that can be achieved by the Wiener filter. It assumes that the restoration is limited by film noise and that the film transmittance values are distributed within a narrow range about T_{av}.

Large values of ϕ_f/ϕ_n specified in the Wiener filter produce more restoration but also more enhancement of noise. An example showing how the amount of restoration of an out-of-focus photograph depends on the value of ϕ_f/ϕ_n assumed in the Wiener filter is given in Fig. 4. This figure shows the original blurred image (upper left) after restoration using 8 different assumed values of ϕ_f/ϕ_n between 10dB and 40 dB. Almost no improvement is evident for a ϕ_f/ϕ_n of 10 dB while increasing the ϕ_f/ϕ_n from 15 dB to 30 dB produces a successively better restoration. Above 35 dB there is excessive enhancement of film noise.

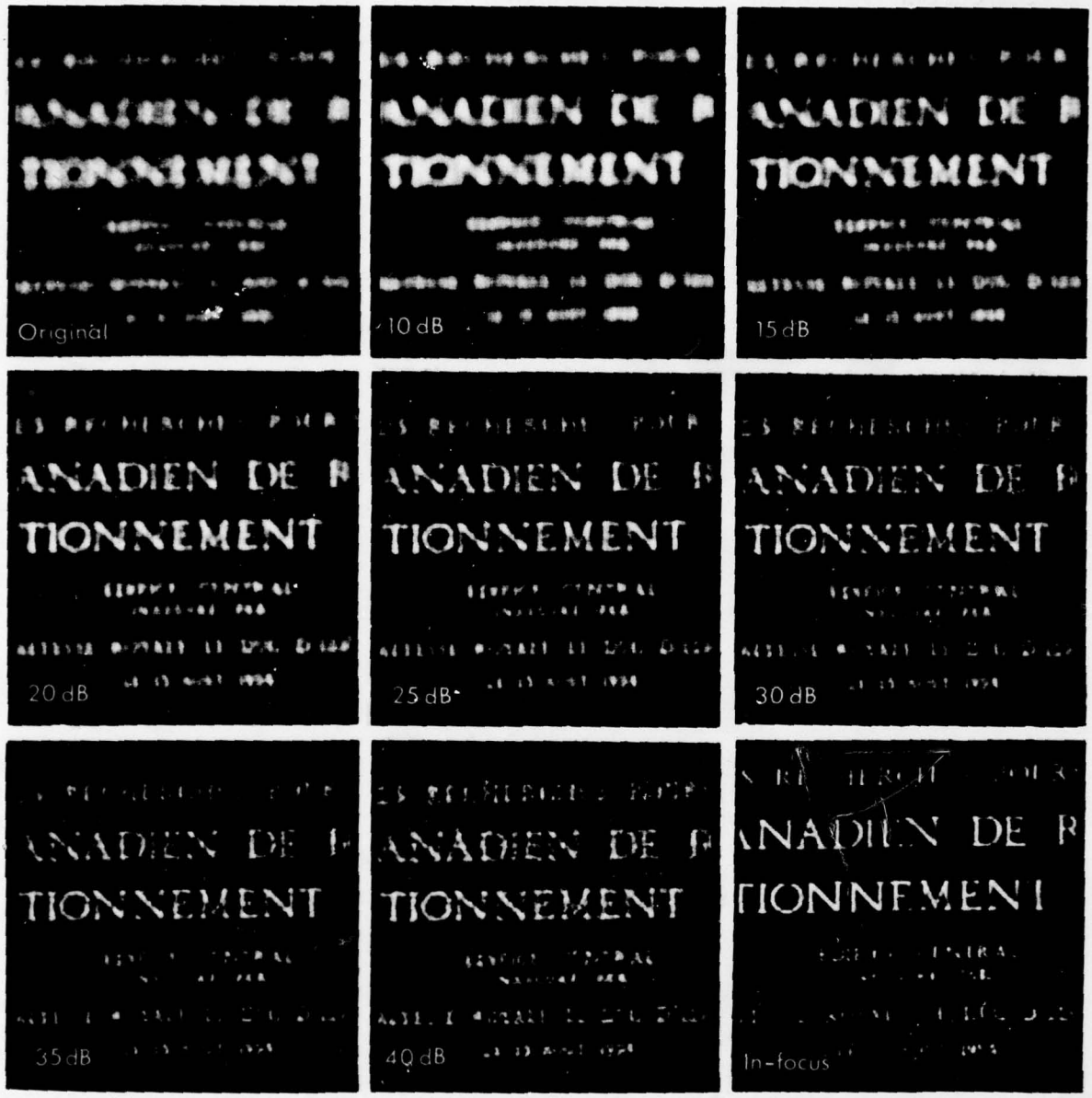

FIGURE 4 Restoration as a function of the value of ϕ_f/ϕ_n specified in the Wiener filter. A region of a photograph taken with the camera out of focus is given in the upper left. The following 7 photographs show the restoration obtained as the value of ϕ_f/ϕ_n (indicated in the lower-left of each restored image) is varied in 5 dB steps from 10 dB to 40 dB. The same region of the sign photographed with the camera in focus is given in the lower right.

In practice, Eq. 18 may best be interpreted as an initial estimate for the value of ϕ_f/ϕ_n to be used in the Wiener filter which can be adjusted to obtain the best restoration. In normal high-contrast photographs, the average transmittance in various regions of the image can differ widely. In this case, no single value of T_{av} will be optimum for all regions of the image. For example, as was explained in Sec. 2.1, the signal-to-noise ratio varies by 4 dB as the film transmittance changes from 0.5 to 0.95. Restoration of a region of a blurred image with average transmittance 0.95 then requires a ϕ_f/ϕ_n 4 dB higher than that of a region with average transmittance 0.5. As illustrated in Fig. 4, a 5 dB difference in the value of ϕ_f/ϕ_n specified in the Wiener filter can have an appreciable effect on the quality of the restoration.

Secondly, the restoration may not be film-noise limited. Other considerations such as the presence of a spatially variant blur (Sec. 3.2) or the attempt to minimize artifacts (e.g. due to film saturation) (Sec. 3.3) may make the use of a value lower than that predicted by Eq. 18 desirable. For lower values of ϕ_f/ϕ_n, the Wiener filter is less sensitive to the use of an incorrect OTF and artifact generation is usually less severe. Depending on the nature of the image to be restored and the information of interest in it, the best restoration may be obtained when a value either higher or lower than that predicted by Eq. 18 is used.

4.0 RESTORATION EXAMPLES

4.1 Simulated Blurs

Assuming complete knowledge of the degradation, the extent to which a blurred photograph can be restored is limited only by the amount of noise which is present. Simulated degradations due to an out-of-focus lens (with circular aperture), linear motion and long-exposure atmospheric transmission were applied to an image as shown in Figs. 5(a), (c) and (e). We introduced the blurs by calculating the 2-dimensional FFT of the ideal transmittance image, multiplying by the appropriate OTF and calculating the inverse FFT. No noise other than that caused by computing errors was added.

The focus blur was assumed to have a PSF consisting of a uniform circular disk of diameter d with an OTF (refs. 9 and 13):

$$H_1(u,v) = \frac{J_1(\pi w d)}{\pi w d} \tag{19}$$

where $J_1(.)$ is the Bessel function of the first kind and first order, and $w^2=u^2+v^2$. The PSF of the linear-motion blur was a line of length l at an angle Θ to the x-axis with an OTF (refs. 9 and 13):

$$H_2(u,v) = \frac{\sin(\pi f l)}{\pi f l} \tag{20}$$

where $f=u\cos(\Theta) + v\sin(\Theta)$. For a long exposure (e.g. 100 ms), the OTF of blurring caused by transmission through atmospheric turbulence is approximately gaussian (ref. 5) and was taken here as:

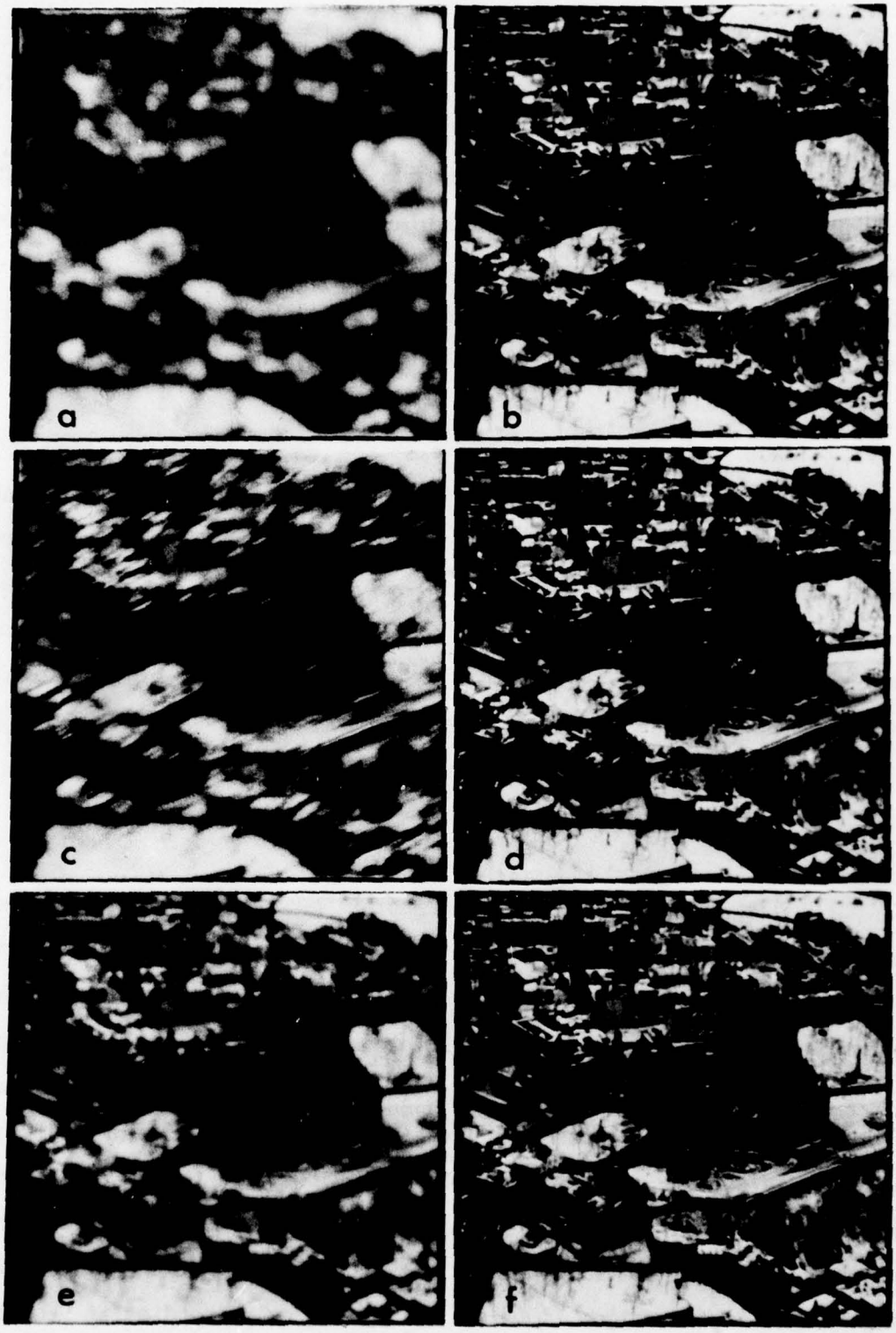

FIGURE 5 Simulated blurs due to (a) an out-of-focus camera, (c) linear motion and (e) long-exposure atmospheric transmission were applied to a photograph. Each blurred image was then restored using a Wiener filter as shown in (b), (d) and (f) respectively. Despite the large amount of blurring present in each case, the low noise level allowed almost complete restoration.

$$H_3(u,v) = \exp[-(b^2w^2/2.155)^{5/6}] \qquad (21)$$

where b is the full width at half maximum of the PSF and $w^2=u^2+v^2$. The modulus of the OTF of each of the 3 blurs (i.e. the modulation transfer function (MTF)) is given in Fig. 6. For the focus blur, d=0.04 x picture width; for the motion blur, l=0.04 x picture width and $\Theta=35°$; and for the atmospheric blur, b=0.01 x picture width.

Each blurred image was restored by calculating the FFT, multiplying by the Wiener filter (with H(u,v) equal to the appropriate OTF and ϕ_f/ϕ_n=50 dB) and calculating the inverse FFT. The restored images are shown in Figs. 5(b), (d) and (f). Despite the large amount of blurring present in each case, the low noise level permitted almost complete restoration. Only the information present in each blurred image was actually used to obtain the restoration.

4.2 Experimental Camera Blurs

Four examples showing the restoration of experimental focus and motion blurs introduced directly in the camera are now given. For both types of degradation, the amount of blurring varies with the distance between the camera lens and the object being photographed. The blurs will then be spatially invariant only if all objects in the photograph are located at the same distance from the camera lens. In addition, spatial invariance of the motion blur requires that the motion be in a plane perpendicular to the optical axis. The first 2 examples show restoration of spatially invariant focus and motion blurs from photographs of flat signs located in a plane perpendicular to the

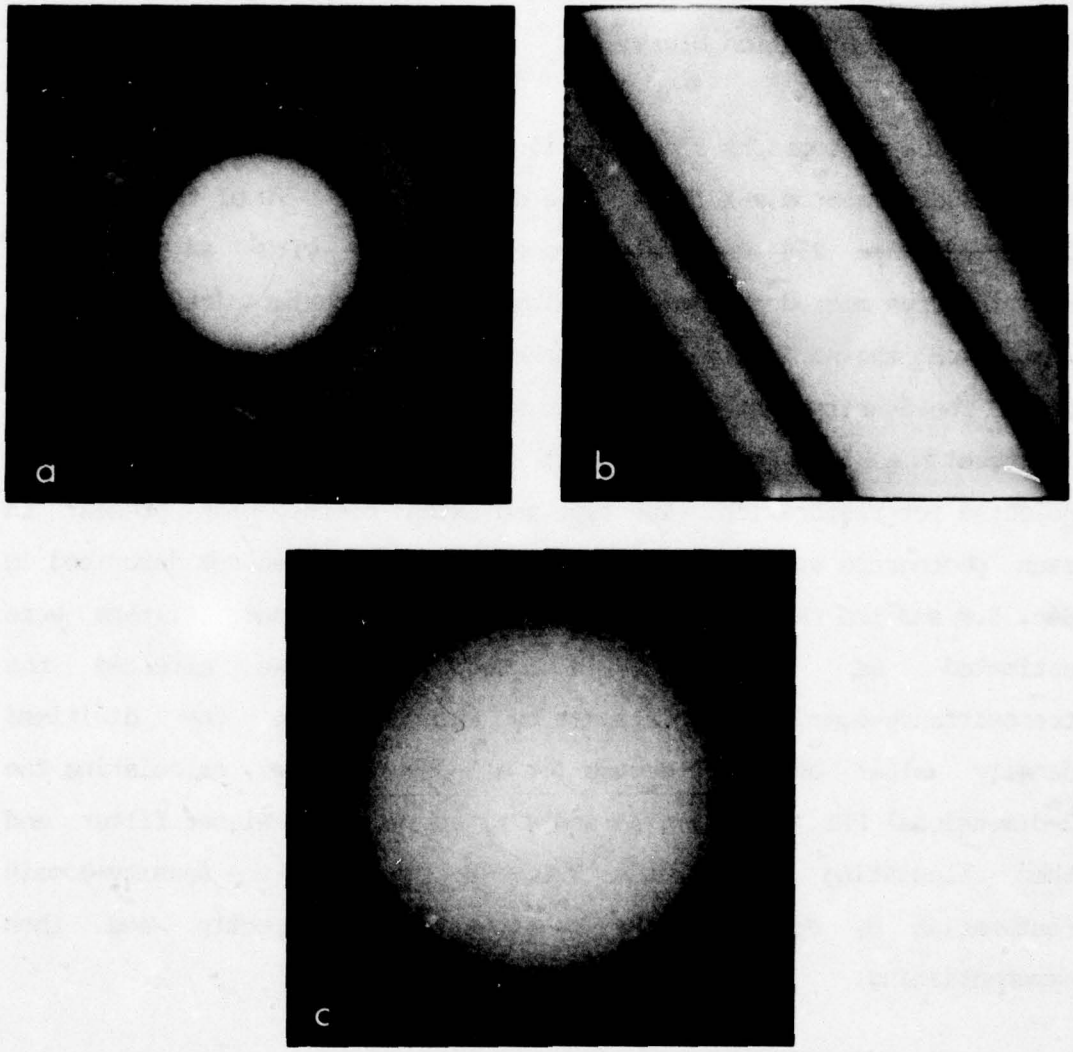

FIGURE 6 The MTF s of the (a) focus, (b) linear-motion and (c) atmospheric blurs present in the images of Fig. 5. The spatial-frequency origin is at the center of each MTF and the 2 axes span the range between plus and minus the Nyquist frequencies.

optical axis where these conditions are approximately satisfied. The third and fourth examples show restoration of photographs containing spatially variant motion blurs.

The photographs shown in Figs. 7, 12, 14 and 21 were taken with 120 mm Kodak Panatomic-X films. The density range 0-2D of the films was digitized into 256 uniformly spaced levels with an Optronics rotating-drum microdensitometer having a 100-μm aperture (ref. 46). The photograph shown in Fig. 13 was taken with a Kodachrome 25 color-slide film. The density range 0-3D of the slide was digitized with a 25 μm aperture. A 512- by 512-element region of each digitized image was selected for restoration. The type and extent of the blur present in each photograph was determined according to the procedures described in Sec. 5.0 and the values of ϕ_f/ϕ_n used in the Wiener filters were estimated as described in Sec. 3.4. We effected the transmittance-domain restorations by exponentiating the digitized density values over a 2-decade (or a 3-decade) range, calculating the 2-dimensional FFT (refs. 17, 45 and 47), applying the Wiener filter and then calculating the inverse FFT. We performed the density-domain restoration by restoring the density values directly and then exponentiating.

We first compare density- and transmittance-domain restorations of a photograph containing a focus blur with a small (approximately 4%) amount of spatial variance. The photograph of a sign taken with the camera out of focus is shown in Fig. 7(a). Using the OTF given by Eq. 19 with a blur-circle diameter of 0.675 mm on the film and ϕ_f/ϕ_n = 25 dB, we restored the image in the density domain (Fig. 7(b)) and in the

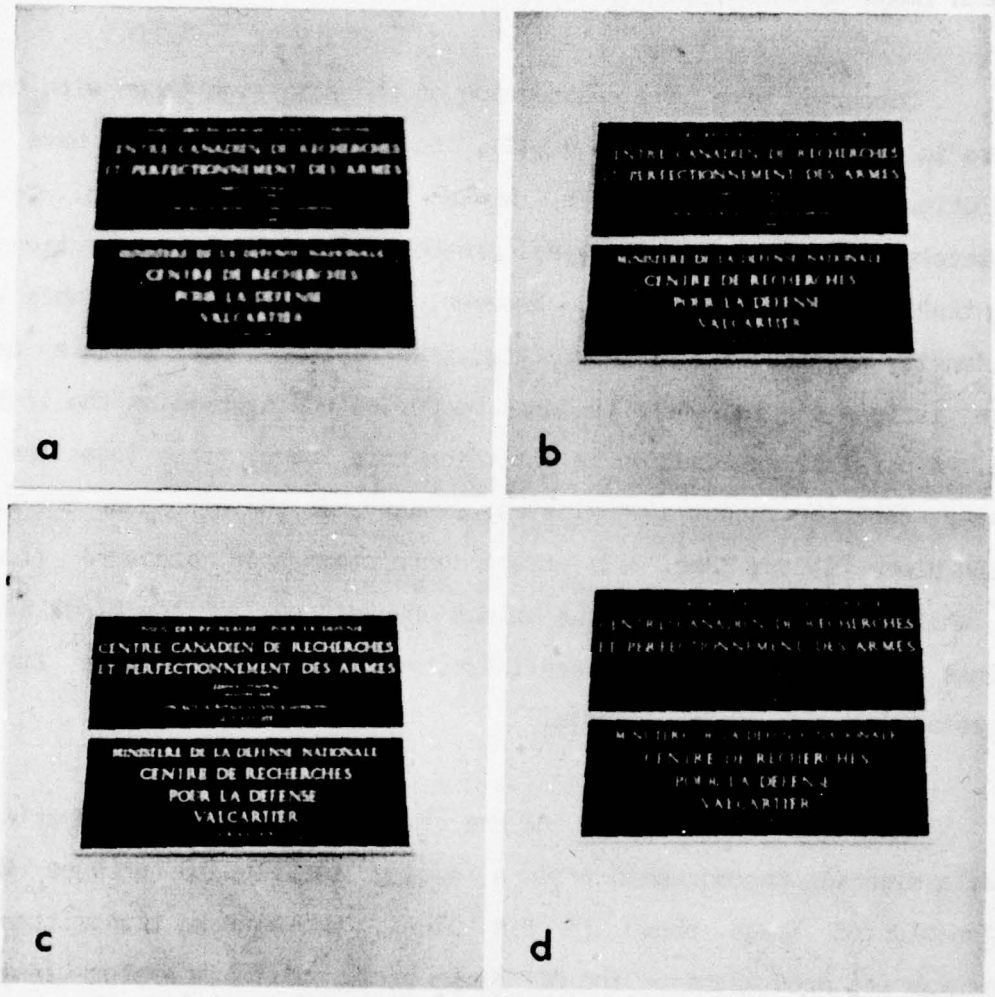

FIGURE 7 A photograph taken with an out-of-focus camera was digitized using a 100-μm raster and a region representing a 5.12-by 5.12-cm area on the original negative is shown in (a). Assuming a ϕ_f/ϕ_n equal to 25 dB and a blur circle with a diameter of 0.675 mm on the negative, a Wiener filter was applied in the transmittance domain (b) and in the density domain (c) to remove the focus blur. A photograph of the same sign taken with the camera in focus is given in (d) to show the resolution limit imposed by the digitization.

transmittance domain (Fig. 7(c)). The central 256- by 256-element region of each image is shown, enlarged, in Figs. 8-10.

Compared with the photograph of the same sign taken with the camera in focus (Figs. 7(d) and 11), both restored images have a resolution close to the limit imposed by the digitization. Text completely illegible in the original can be read in both restorations. The transmittance restoration, however, may be slightly preferable to the density restoration. In particular, the text is more legible and there is less ringing where the dark border of the sign joins the light wall. A possible explanation is that, for this image, the logarithmic density function is not approximately linear over the extent of the PSF of the Wiener filter (Sec. 3.2) at the sharp changes in exposure (i.e. the white letters against the black background and the black sign against the white wall). This nonlinearity only occurs when the image is restored in the density domain.

As a second example of the removal of a spatially invariant blur, a sign was photographed from a moving vehicle to produce the motion-blurred image shown in Fig. 12(a). The blurred transmittance image was restored assuming the OTF given by Eq. 20 (with a blur length of 1.43 cm on the film and $\Theta = 0°$) taking $\phi_f/\phi_n = 30$ dB. The result is given in Fig. 12(b). Despite its large extent (greater than 1/4 of the picture width), the motion blurring of the sign has been almost completely removed by the restoration.

In the third example, the original photograph (Fig. 13(a)) consists of 2 areas: one contains no degradation, the other contains

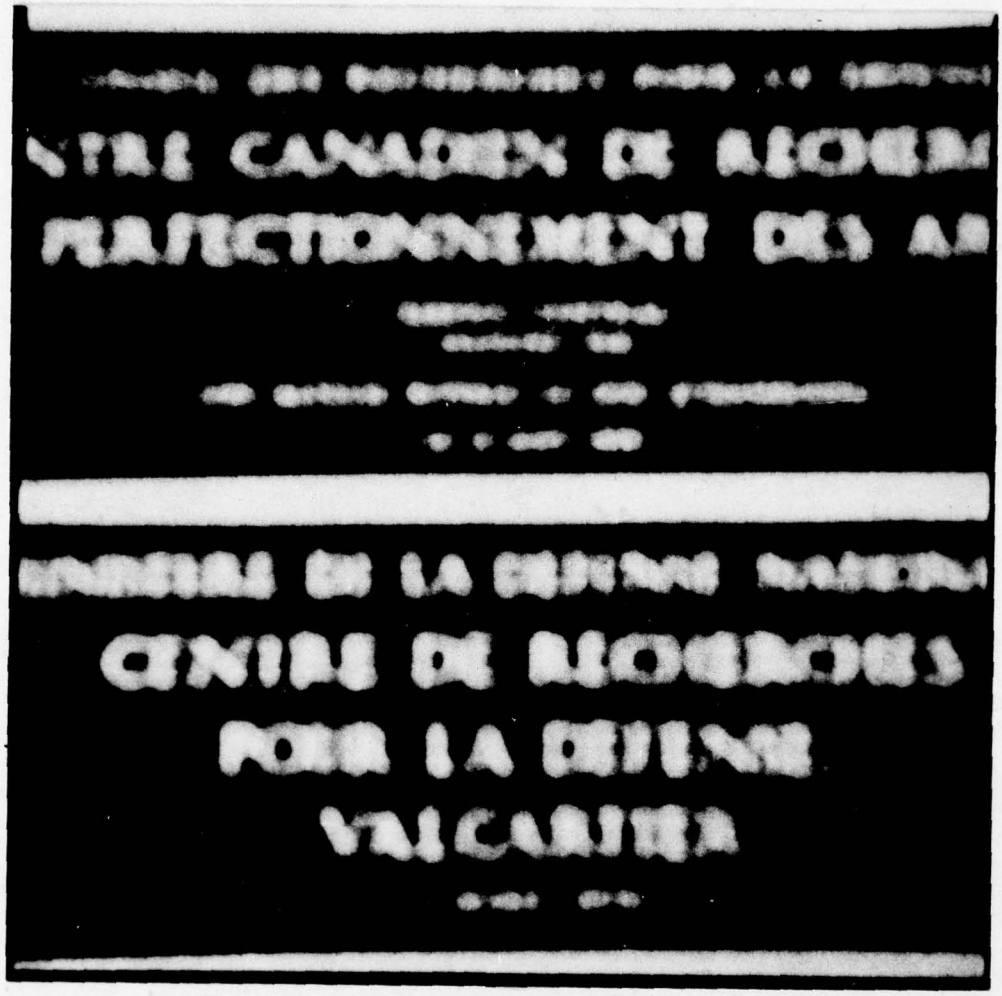

FIGURE 8 Enlargement showing the central region of a blurred photograph (Fig. 7(a)) taken with the camera out of focus

FIGURE 9 Transmission-domain restoration of the blurred image shown in Fig. 8

FIGURE 10 Density-domain restoration of the blurred image shown in Fig. 8

FIGURE 11 The region of the sign given in Fig. 8 photographed with the camera in focus

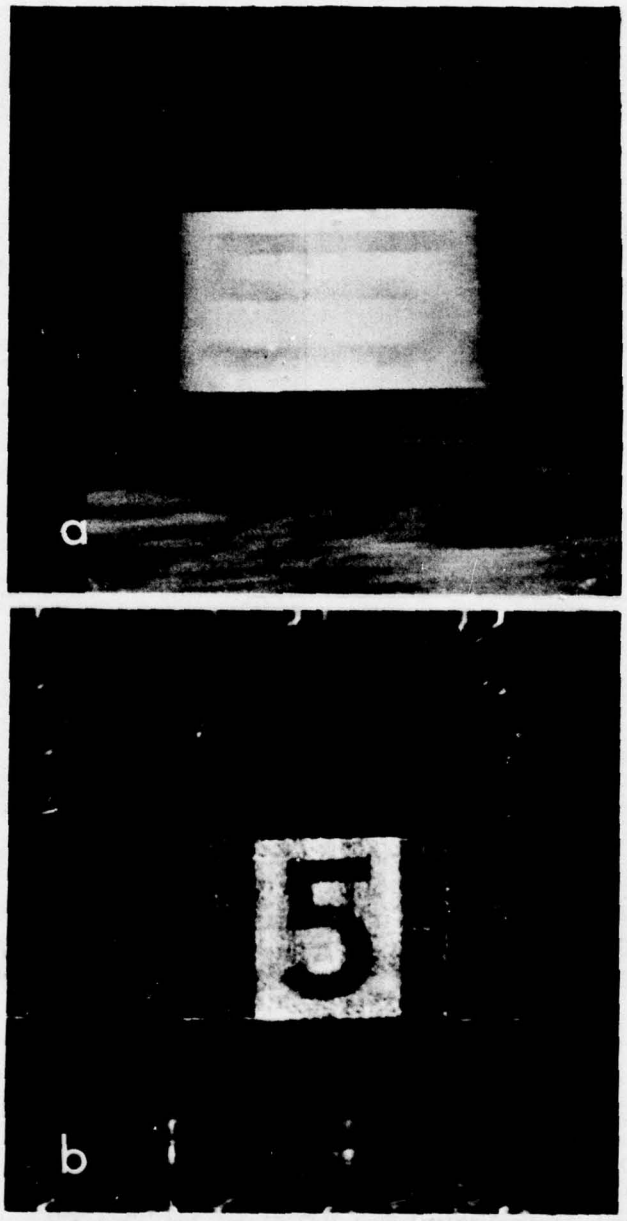

FIGURE 12 Restoration of a photograph containing spatially invariant motion blur. The original blurred image (a) is shown after restoration in (b).

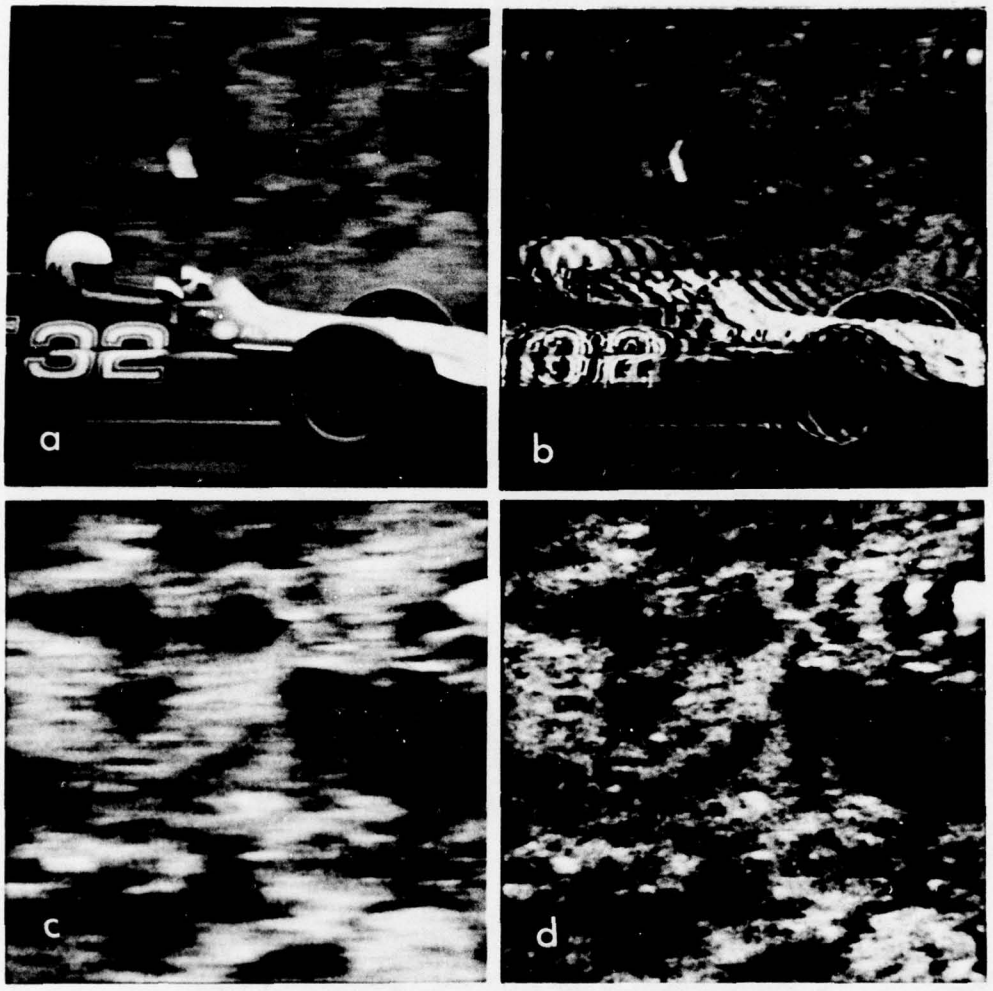

FIGURE 13 The background region of the photograph (a) is degraded by linear-motion blur. The result of restoring the complete photograph to deblur the background is given in (b). Enlargements showing a region of the background before and after restoration are given in (c) and (d). Artifacts due to restoration of the unblurred portion of the image and to film saturation are apparent in (b).

linear-motion blur. The camera tracked the moving vehicle so the image of the vehicle was correctly recorded while the image of the stationary background was blurred. The result of restoring the complete image to remove the blurring from the background is shown in Fig. 13(b). We restored the image in the transmittance domain using the OTF given by Eq. 20 with a blur length of 0.61 mm on the film, $\Theta = 0°$ and $\phi_f/\phi_n = 20$ dB. Enlargements showing a section of the background region before and after restoration (Figs. 13(c) and 13(d)) illustrate that the blurring has been effectively removed. For example, features which appear as streaks in the original image can readily be identified as small rocks after restoration, and boundaries between light and dark areas have been sharpened. (The background consists of an almost-vertical bank of earth.)

Two types of artifacts are evident in the restored image. Both appear as severe ringing in which the PSF of the Wiener filter is displayed. (Compare the ringing with the PSF of the Wiener filter given in Fig. 3(e).) The first type of artifact is caused by application of the Wiener filter to the unblurred image of the vehicle. The second is due to film saturation in 2 over-exposed areas of the image (in particular in the wedge-shaped feature close to the center of Fig. 13(a) and in the area in the upper-right corner). One can reduce or eliminate these artifacts by editing the image before restoration to remove the over-exposed areas (i.e. by matching the average gray level of the area to that of the surrounding region), and by confining the restoration to the motion-blurred portion of the image (i.e. by selecting a region which does not include the vehicle).

The fourth image to be restored (Fig. 14(a)) is degraded by spatially variant motion blur. The scene, which was photographed from a moving vehicle, contained objects located at different ranges from the camera. In addition, the camera was not moving in the plane perpendicular to the optical axis. Both the length and direction of the blur therefore varied throughout the image. The result of restoring the front of the building (using a blur length of 1.18 mm on the film, Θ = 37.5° and ϕ_f/ϕ_n = 20 dB) is given in Fig. 14(b). Enlargements showing the regions of the sign and the door before and after restoration are given in Fig. 15. Comparison with the unblurred photograph of the building (Fig. 14(c)) obviously shows that text which is illegible in the original blurred image has been correctly restored. For example, after restoration, the street number "382" on the door can be read in Fig. 15(d) as can the telephone number "843-6652" in Fig. 15(c).

Other objects in the photograph, e.g. the car to the left of the building and the chimney on the building, are located further from the camera and are not correctly restored. The artifacts (PSF ringing) generated by incorrect restoration of these objects do not extend significantly into the correctly restored regions. Ringing of 2 highlights on the car where the film has saturated is also evident in the restored image.

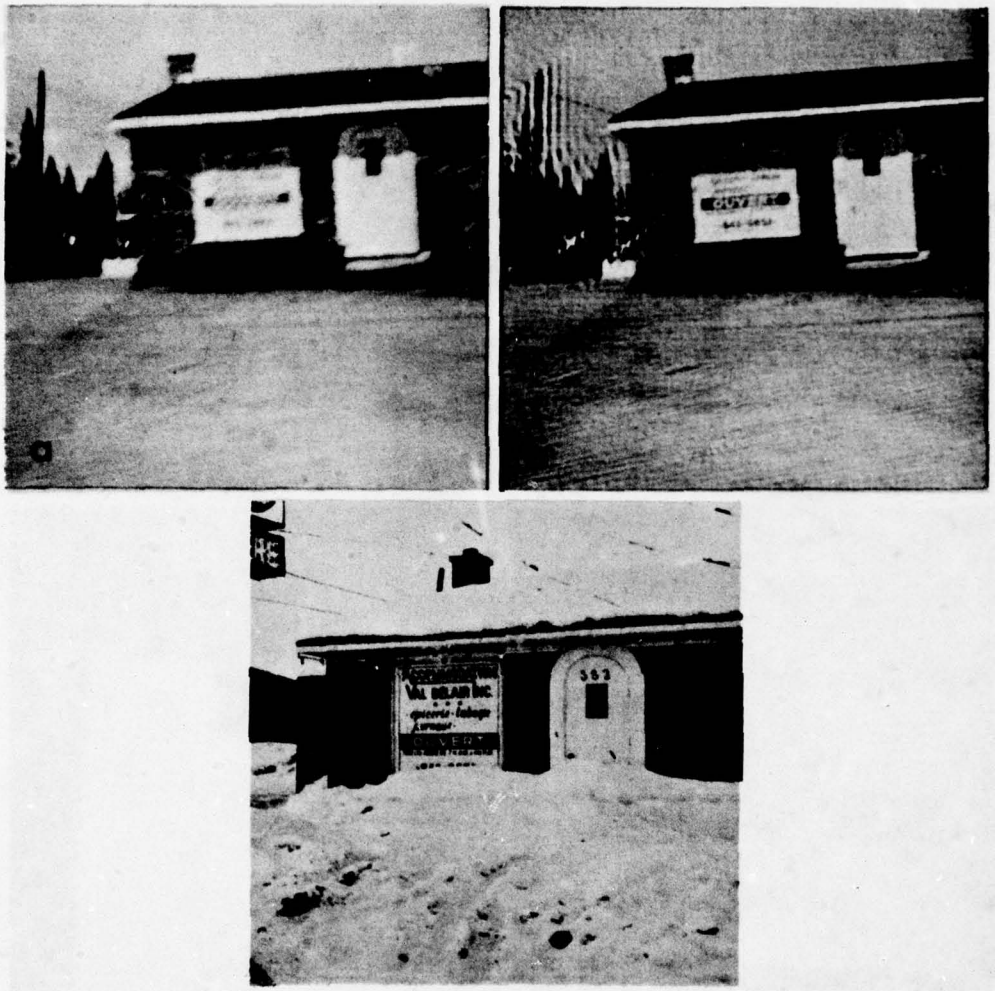

FIGURE 14 Restoration of a photograph containing spatially variant motion blur. The original blurred image (a) is shown in (b) after restoration of the front of the building. Other regions of the image are incorrectly restored. An unblurred photograph of the building is given in (c).

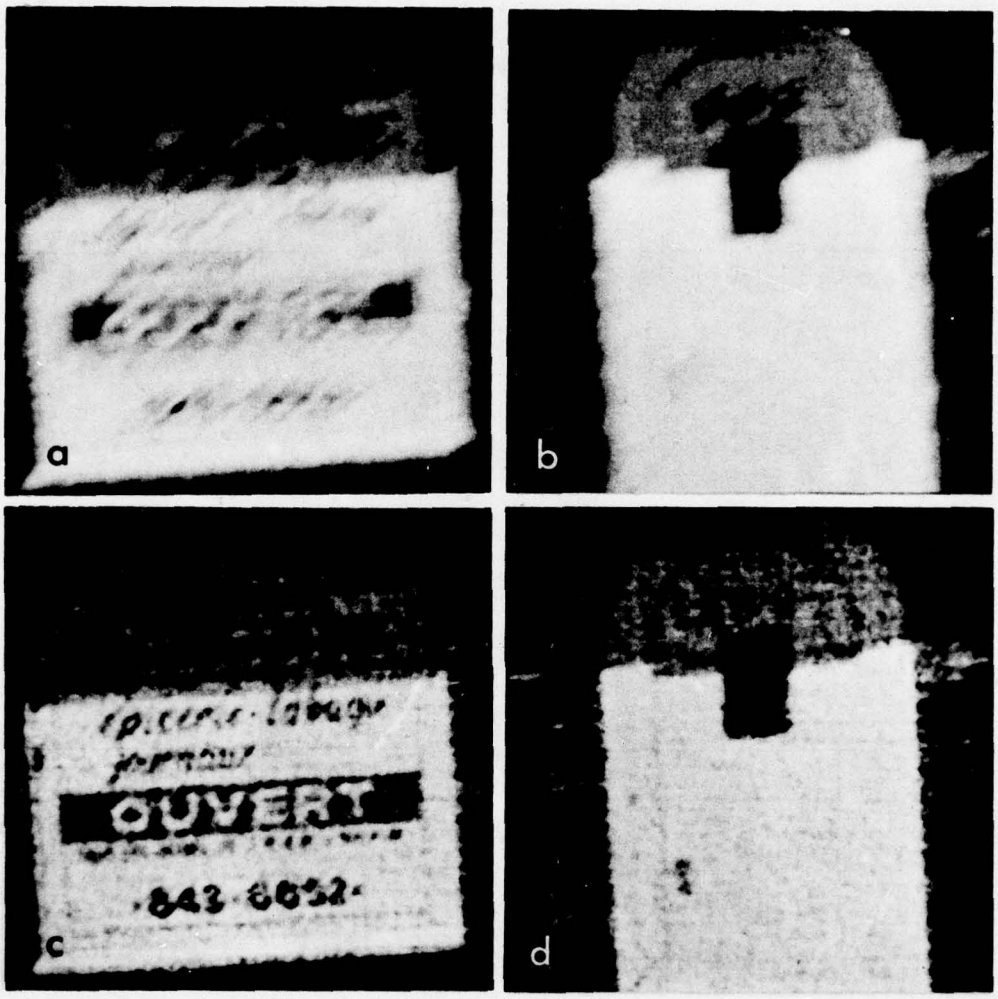

FIGURE 15 Enlargements of the images given in Figs. 14(a) and (b) showing the region of the sign (a) before and (c) after restoration, and the region of the door (b) before and (d) after restoration

5.0 DETERMINATION OF THE OTF

5.1 Interactive Method

To restore a blurred image with a Wiener filter, one must know the OTF as given by the type of blur (e.g. out-of-focus) and its extent (e.g. diameter of blur circle). The present section shows how this can be determined interactively. A second method for determining the required information which consists in analysing the power spectrum of the blurred image and which can be applied for certain types of OTFs, is described in Sec. 5.2.

In the interactive method, a small region of the complete image is selected and restored using guesses for the type and extent of the blur. The initial guesses are improved (usually by systematically repeating the restoration as a function of a single parameter such as blur-circle diameter) and the values which subjectively yield the best result are used to restore the complete image.

The initial guesses for the type and extent of the blur can be based both on a priori knowledge and on direct analysis of the blurred image. For example, in restoring the image of Fig. 13 we assumed a priori that the background was blurred by linear-motion degradation. (The moving vehicle was not blurred, which indicated correct tracking of the camera. Over the 1/250 s exposure time, the camera motion relative to the stationary background is then approximately linear.) We obtained initial estimates for the length and direction of the motion blur by measuring the extent of the blurring of objects in the background that were assumed to contain point or edge structure (ref. 5).

An example showing variation of a parameter from the initial estimate to optimize the restoration is given in Fig. 16. Here, we restored a region of the out-of-focus photograph of a sign shown in Fig. 7(a) using 8 different assumed values for the diameter of the blur circle on the negative. The values varied in 0.025 mm steps from 0.575 mm to 0.825 mm. It is evident that the best restoration is obtained for a blur circle diameter of 0.675 mm. This value was used to restore the complete image as shown in Figs. 7(b), 7(c), 9 and 10.

5.2 Power Spectrum Analysis

According to Eq. 15, one may express the blur in the spatial-frequency domain by multiplying the discrete Fourier transform of the ideal image by the OTF. The MTF of certain degradations can consist of a well-defined pattern. For example, the MTF of the focus blur given in Fig. 6(a) contains characteristic ring structure while the MTF of the linear motion blur given in Fig. 6(b) contains characteristic linear structure. Provided that it is not obscured by the noise term in Eq. 15 or by structure in the discrete Fourier transform of the ideal image, the MTF of the blur will appear in the power spectrum of the degraded image. Gennery (ref. 13) has shown that in some cases (particularly if the MTF of the blur has zeros) this pattern can identify both the type and the extent of the blur.

As an example of this, four regions of the out-of-focus photograph of the sign shown in Fig. 7(a) were selected (Fig. 17) and the power spectrum (i.e. the modulus of the FFT) of each was calculated (Fig. 18). The ring structure present in each power spectrum is

FIGURE 16 Determination of the OTF of the blur interactively. A region of a blurred photograph is shown in the upper left. Assuming the blur is due to an out-of-focus camera, the image was restored using 8 different assumed values of blur-circle diameter. These values, which are written in the lower left of each image, varied in 0.025 mm steps from 0.575 mm to 0.750 mm. The restoration is clearly optimum for a blur-circle diameter of 0.675 mm.

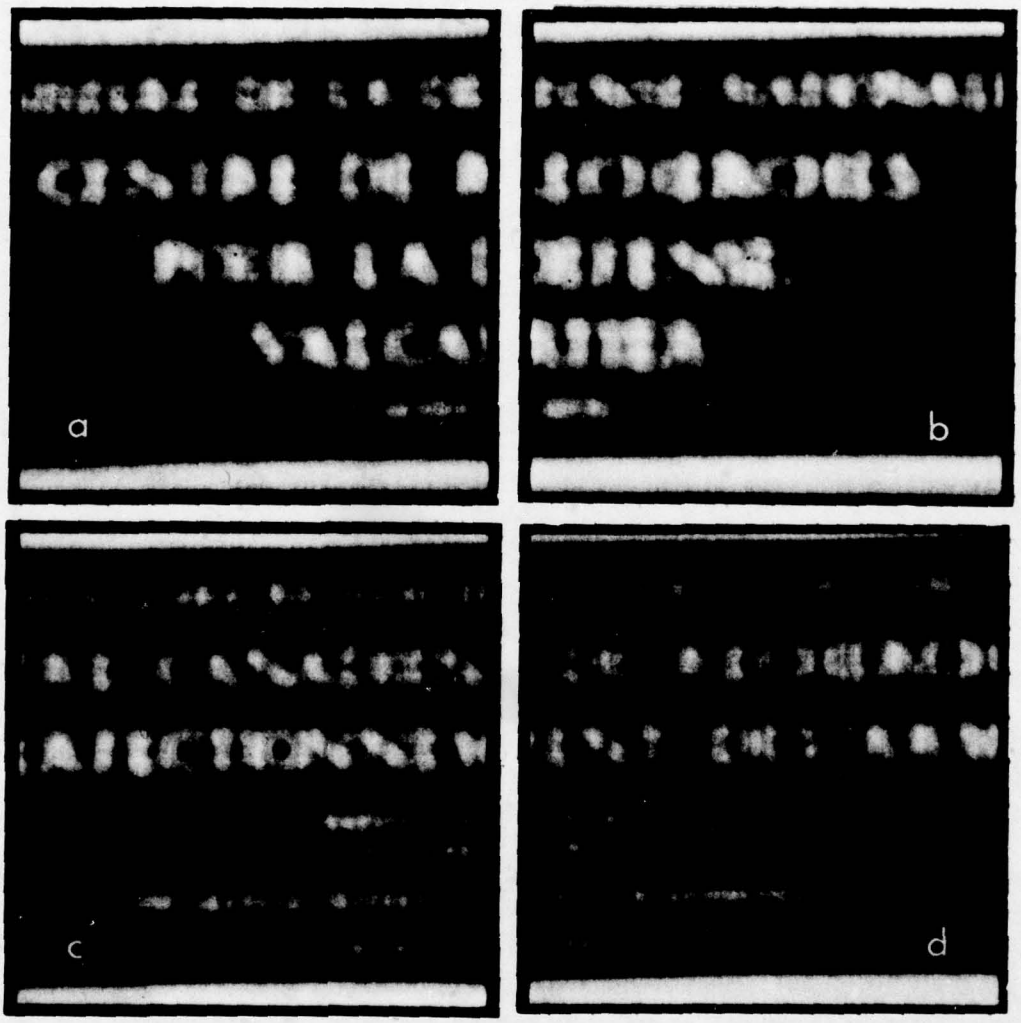

FIGURE 17 Four regions of the photograph of a sign taken with the camera out of focus are shown in (a), (b), (c) and (d)

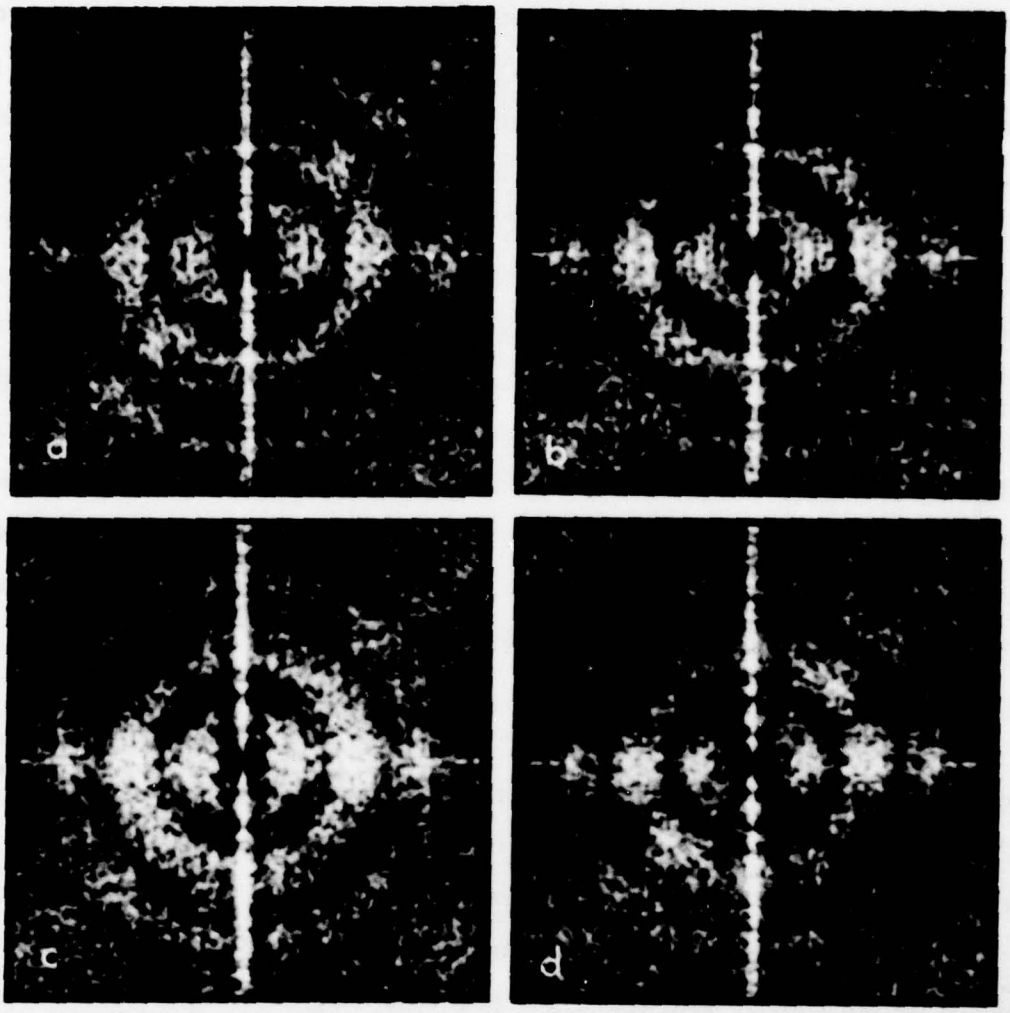

FIGURE 18 Identification of the MTF of the blur by power spectrum analysis. The power spectra of 4 regions of a photograph taken with an out-of-focus camera (i.e. the 4 images given in Fig. 17) are shown in (a), (b), (c) and (d). While each of the 4 images before blurring contains different spatial features the same ring structure, which is characteristic of the out-of-focus blurring, is evident in all power spectra.

characteristic of the focus degradation. Following Eq. 19, the OTF of the focus degradation is a Bessel function of the first kind and first order with argument $w=(u^2+v^2)^{1/2}$ divided by w. This function is circularly symmetric about the frequency origin with the first 4 zeros located at $w_1=1.220/d$, $w_2=2.234/d$, $w_3=3.238/d$ and $w_4=4.242/d$, where d is the diameter of the blur circle. The zeros in the MTF occur at the same locations. By summing the power in ring-shaped regions about the origin, dividing by the area of each region and plotting this as a function of distance from the spatial-frequency origin (Fig. 19), one can determine the locations of the first 3 minima in each power spectrum (corresponding to the first 3 zeros in the Bessel-function OTF). Each minimum in the radial power distributions appearing in Fig. 19 gives an estimate for the diameter of the blur circle. Averaging the 3 values obtained from each graph gives the following estimates for the average blur-circle diameters: region (a), d=0.67 mm; region (b), d=0.66 mm; region (c), d=0.69 mm; region (d), d=0.69 mm.

This method can be very accurate. Here it was able to detect the fact that the upper portion of the sign (regions (a) and (b)) was 4% less out-of-focus than was the bottom portion (regions (c) and (d)). The photograph was taken with the camera focused at a point behind the sign and, as is evident in Fig. 7(a), the lower portion of the sign was closer to the camera than the upper portion.

Before calculating the above power spectra, we high-pass filtered each image using a digital approximation to the two-dimensional Laplacian operator (refs. 5 and 13):

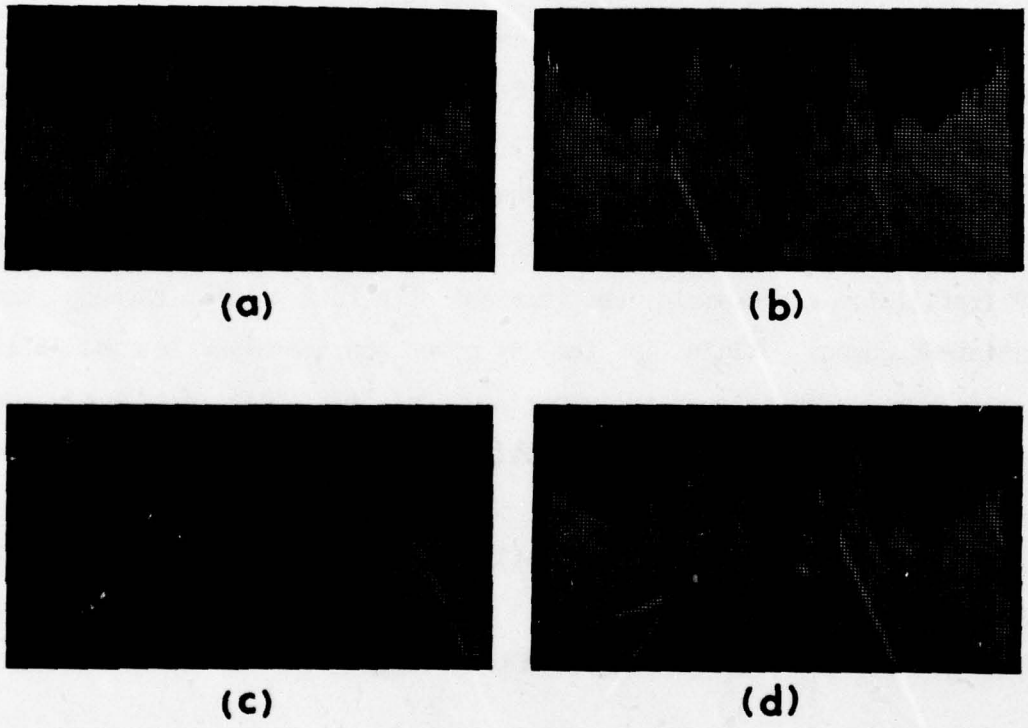

FIGURE 19 The radial power distributions of the 4 power spectra given in Fig. 18. The oscillation present in each distribution is characteristic of the focus blurring and each minimum gives an estimate for the diameter of the blur circle. The graphs (a), (b), (c) and (d) respectively yield average values of 0.67 mm, 0.66 mm, 0.69 mm and 0.69 mm for the diameter of the blur circle on the film negative.

$$g'(x,y) = g(x-1,y) + g(x+1,y) + g(x,y-1) + g(x,y+1) - 4g(x,y) \quad (22)$$

This filter enhances the low-amplitude higher spatial frequencies approximately as u^2+v^2, which makes the MTF pattern more easily visible in the power spectrum.

When the power spectrum is estimated as the modulus of the FFT, a discontinuity effectively exists if the opposite edges of the image do not match one another (refs. 15, 26 and 36). This discontinuity introduces spatial-freguency components along the vertical and horizontal axes of the power spectrum which are not multiplied by the MTF (ref. 13). For example, the vertical structure passing through the spatial-frequency origin in the 4 power spectra given in Fig. 18 is caused by mismatch between the upper and the lower edges in each of the corresponding images shown in Fig. 17. Eliminating these undesired axial spatial frequencies before calculating the radial power distributions of Fig. 19 (by setting the appropriate regions of each power spectrum to zero) significantly improved the accuracy with which the positions of the minima could be determined.

In general, the power spectra of different regions of the ideal image will have different structure but all will be multiplied by the same MTF (assuming a spatially invariant degradation). Then averaging the power spectra of different regions of the image can enhance the MTF pattern. Averaging the 4 power spectra of Fig. 18 gave the enhanced MTF pattern shown in Fig. 20(a).

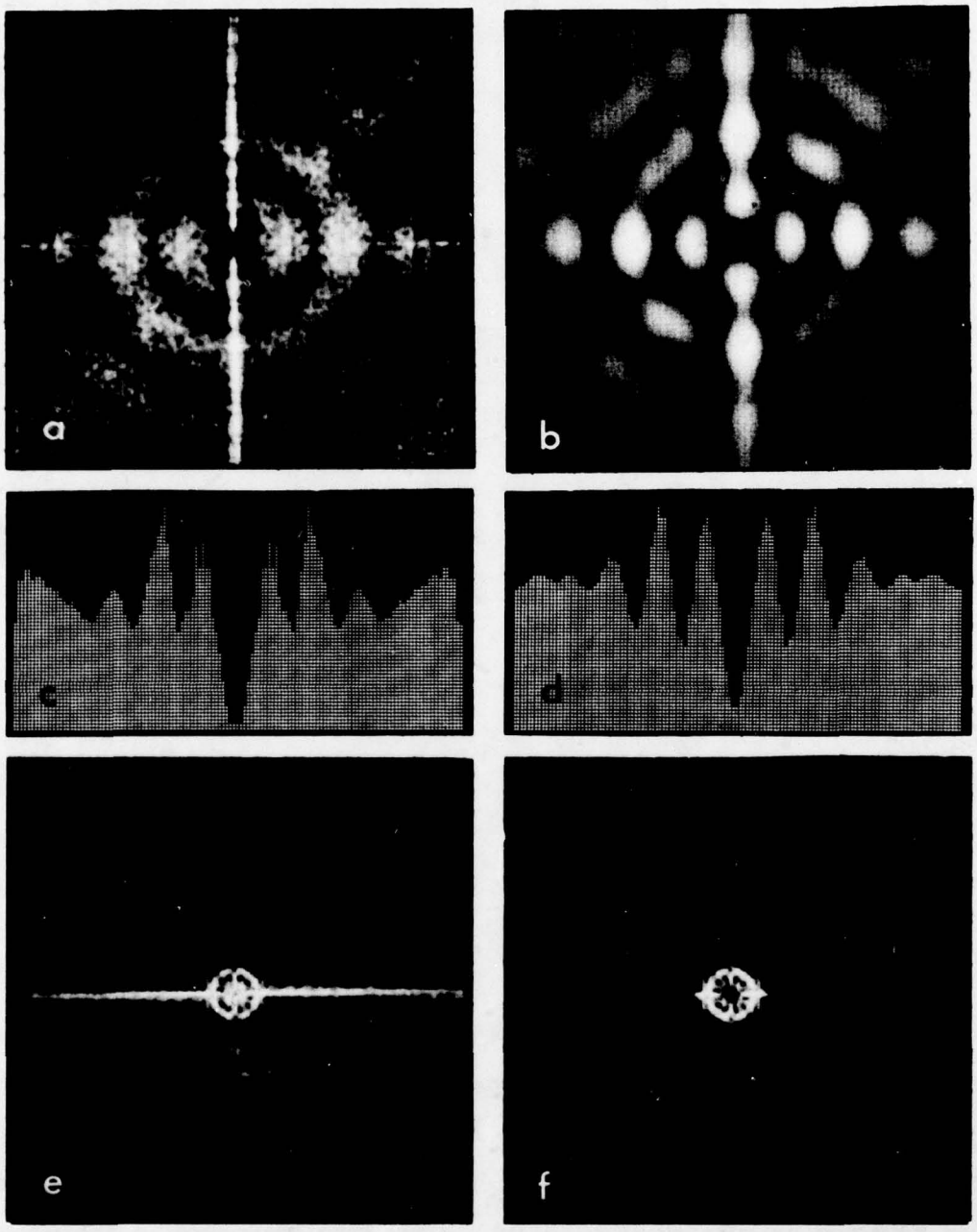

FIGURE 20 Enhancement of the MTF pattern in the power spectrum of a blurred photograph by 2 methods. In (a) the enhancement was obtained by averaging the power spectra of 4 different regions of the blurred image. Further enhancement was obtained in (b) by band-pass filtering the averaged power spectrum (a). The power spectrum of (a) is shown before filtering in (e) and after filtering in (f). The radial power distributions of (a) and (b) are given in (c) and (d) respectively.

If the approximate nature of the blur is known, then a spatial filter can be applied to the power spectrum of the degraded image to further enhance the MTF pattern. However, the filter must be chosen so that it does not distort the desired MTF pattern or introduce additional structure. The power spectrum of the averaged power spectrum given in Fig. 20(a) is shown in Fig. 20(c). It is evident that the energy corresponding to the MTF of the present blur is concentrated within a narrow annular range about the spatial-frequency origin. This corresponds to the fundamental frequency of the Bessel function. Band-pass filtering the power spectrum given in Fig. 20(a) so as to retain only these spatial frequencies considerably enhances the MTF pattern, as shown in Fig. 20(b). The power spectrum of the power spectrum after band-pass filtering is given in Fig. 20(f). Only 3 minima are present in the radial power distribution before filtering (Fig. 20(c)) while after filtering a fourth minimum is apparent (Fig. 20(d)). Before filtering the minima in the power spectrum yield an average blur-circle diameter d=0.68 mm while after filtering the value d=0.72 mm is obtained. The filtering has therefore only slightly altered the positions of the minima.

We conclude this section with an example which summarizes the use of the above procedures to restore the blurred photograph shown in Fig. 21(a). The central 256- by 256-element region of the digitized photograph was selected, a Laplacian high-pass filter applied and the power spectrum calculated (Fig. 21(b)). The ring structure in the power spectrum identifies the blur as being due to an out-of-focus camera (with circular aperture), and the first 3 minima yield estimates of 1.72 mm, 1.74 mm and 1.77 mm for the diameter of the blur circle on the

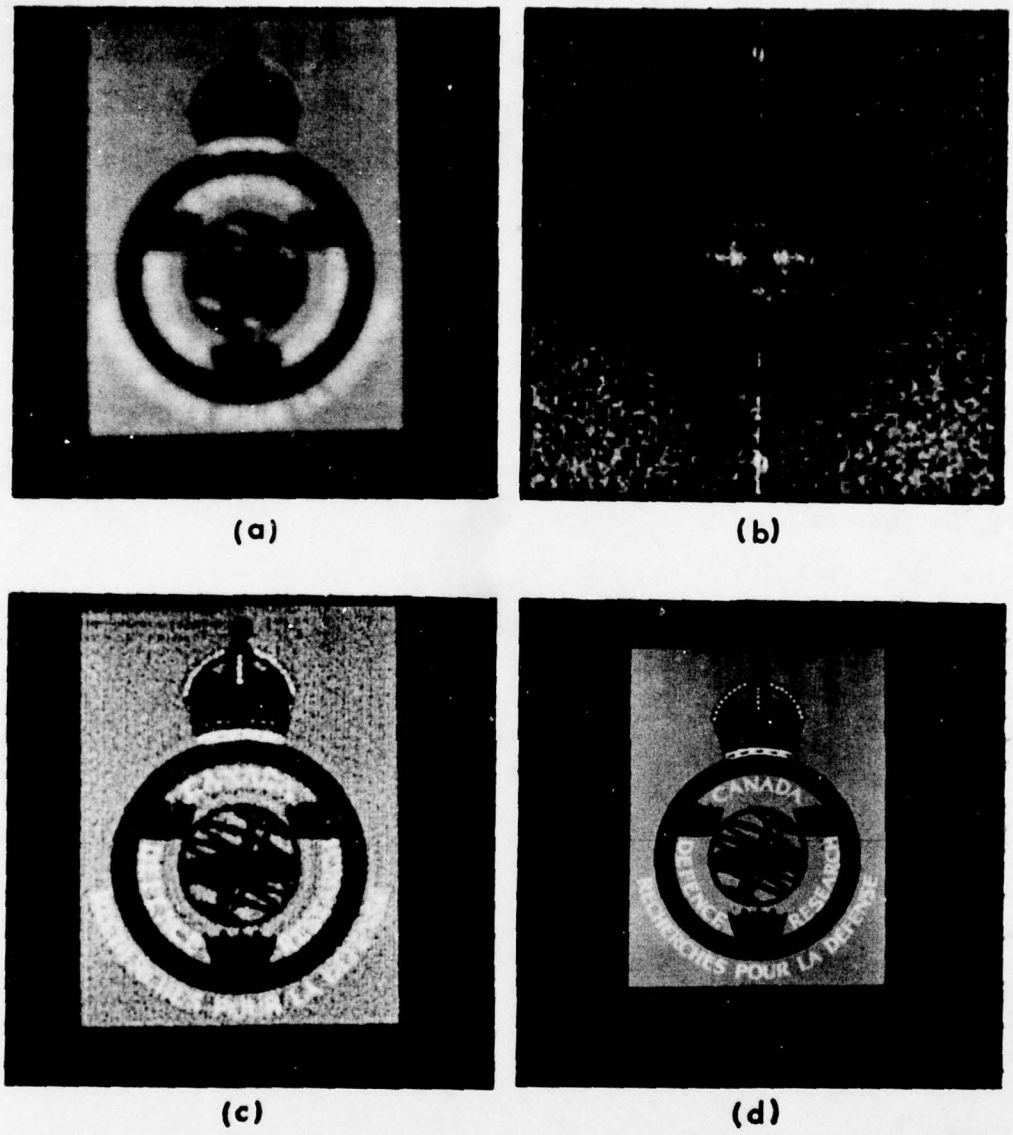

FIGURE 21 Summary of the procedure used to restore the blurred image (a). The power spectrum of the image (b) contains ring structure which identifies the blurring as being due to an out-of-focus camera with a blur-circle diameter of 1.76 mm on the film negative. Assuming this OTF, the image was restored using a Wiener filter as shown in (c). The same insignia photographed with the camera in focus (d) verifies the correct restoration of details not resolved in the original blurred image.

negative. Measurement of the RMS noise in uniformly exposed regions of the photograph indicated that a picture element with transmittance Ø.5 would have a signal-to-noise ratio of 23 dB. Using a ϕ_f/ϕ_n equal to 25 dB and assuming a blur-circle diameter of 1.75 mm, we restored the image in the transmittance domain with the OTF given by Eq. 19. The result is shown in Fig. 21(c). The photograph of the same insignia taken with the camera in focus (Fig. 21(d)) verifies the correct restoration of details not evident in the original blurred image (e.g. the beads in the crown and structure within the central circle). The resolution (size of the smallest detail that can be resolved) has been increased by a factor of 5 by the restoration.

6.0 CONCLUSIONS

Because of excessive computing times, it is not practical to use many of the existing digital restoration procedures to deblur high-resolution images. Wiener filtering, implemented in the spatial-frequency domain that uses an FFT algorithm, is one approach which can be applied to restore high-resolution images (e.g. images containing 512 by 512 elements) and which uses only moderate computational facilities.

A complete Wiener-filtering restoration procedure, including 2 methods for identifying the blur that analyse the blurred image directly using only limited a-priori knowledge, was described here. Examples showing the restoration of experimental focus and motion blurs were given. The blurs were introduced directly in the camera and normal "amateur" photographic films and cameras were used.

Correct application of the Wiener filter, and in particular a knowledge of its limitations, is fundamental to obtaining an acceptable restoration. These limitations were described in detail with regard to restoration of blurred photographs. Techniques for restoring blurred photographs which take account of the properties of the Wiener filter as well as other practical considerations (e.g. film nonlinearity, artifact generation, edge effects etc.) were described.

The most serious disadvantages of a Wiener filter are that it can only restore blurs containing a small amount of spatial variance, it does not simultaneously assume the correct models for film noise and for

the blurring, and it does not make use of known physical constraints (e.g. the ideal image cannot contain negative values or be infinite). It incorrectly assumes that the signal-to-noise ratio of the film is independent of exposure. Furthermore, the restoration is linear (and therefore sub-optimum (ref. 1)) and is based on minimizing the mean-square error between the ideal and the restored images. It is doubtful whether the mean-square error criterion correlates well with subjective estimates of image quality (refs. 2 and 29). (Many of the other restoration procedures suffer the same shortcomings however.)

The present report has demonstrated that, in situations of practical interest, significant restorations of high-resolution blurred photographs can be obtained through the proper use of an inverse Wiener filter. The techniques described here have recently been applied to the more difficult problem of restoring blurred photographs taken under poor conditions. Useful improvements in resolution have been obtained despite incorrect film exposure and high film granularity which occurred in several of the photographs.

Methods are being investigated to improve the subjective quality of the Wiener-filter restorations, to increase the range of OTFs that can be restored and to decrease the computing times required. In particular, Hunt (ref. 2) has demonstrated that inclusion of the frequency response of human vision in the Wiener filter produces improved results. Provision to specify the OTF as a 2-dimensional discrete Fourier transform rather than only as an analytic function would allow blurs with arbitrary PSFs to be restored. The present restoration procedure will be implemented on a PDP 11/40 minicomputer

interfaced to an array processor with a large data memory. Compared to the present software implementations, the array processor will decrease the time required to transform and filter the image by 2 orders of magnitude.

7.0 ACKNOWLEDGEMENTS

It is a pleasure to thank Mr P.-E. Boutin for useful discussions and for help in setting up the present image display system. I also wich to thank Mr A. Pépin and Mr J.-C. Ruelland for their able programming assistance. Experiments simulating the restoration procedure were performed by Mr J.-M. Bordua. The 2-dimensional FFT routines were written by Mr L. Sévigny.

8.0 REFERENCES

1. Frieden, B. R., "Image Enhancement and Restoration", in Picture Processing and Digital Filtering, edited by T. S. Huang, Springer-Verlag, New York, 1975, pp. 177-248.

2. Hunt, B. R., "Digital Image Processing", Proc. IEEE, Vol. 63, pp. 693-708, April 1975.

3. Andrews, H. C., "Digital Image Restoration: A Survey", IEEE Computer, Vol. 7, pp. 36-45, May 1974.

4. Sondhi, M. M., "Image Restoration: The Removal of Spatially Invariant Degradations", Proc. IEEE, Vol. 60, pp. 842-853, July 1972.

5. Huang, T. S., Schreiber, W. F. and Tretiak, O. J., "Image Processing", Proc. IEEE, Vol. 59, pp. 1586-1609, November 1971.

6. Oppenheim, A. V., Schafer, R. W. and Stockham, T. G. Jr., "Nonlinear Filtering of Multiplied and Convolved Signals", Proc. IEEE, Vol. 56, pp. 1264-1291, August 1968.

7. Stockham, T. G. Jr., Cannon, T. M. and Ingebretsen, R. B., "Blind Deconvolution Through Digital Signal Processing", Proc. IEEE, Vol. 63, pp. 678-692, April 1975.

8. Oppenheim, A. V., Kopec, G. E. and Tribolet, J. M., "Signal Analysis by Homomorphic Prediction", IEEE Trans. Acoustics, Speech and Signal Processing, Vol. ASSP-24, pp. 327-332, August 1976.

9. Cannon, M., "Blind Deconvolution of Spatially Invariant Image Blurs with Phase", IEEE Trans. Acoustics, Speech and Signal Processing, Vol. ASSP-24, pp. 58-63, February 1976.

10. Hunt, B. R., "The Application of Constrained Least Squares Estimation to Image Restoration by Digital Computer", IEEE Trans. on Computers, Vol. C-22, pp. 805-812, September 1973.

11. Helstrom, C. W., "Image Restoration by the Method of Least Squares", J. Opt. Soc. Am., Vol. 57, pp. 297-303, March 1967.

12. Pratt, W. K., "Generalized Wiener Filtering Computation Techniques", IEEE Trans. Comp., Vol. C-21, pp. 636-641, July 1972.

13. Gennery, D. B., "Determination of Optical Transfer Function by Inspection of Freguency-Domain Plot", J. Opt. Soc. Am., Vol. 63, pp. 1571-1577, December 1973.

14. Walkup, J. F. and Choens, R. C., "Image Processing In Signal-Dependent Noise", Opt. Eng., Vol. 13, pp. 258-266, May-June 1974.

15. McDonnell, M. J. and Bates, R. H. T., "Preprocessing of Degraded Images to Augment Existing Restoration Methods", Computer Graphics and Image Processing, Vol. 4, pp. 25-39, 1975.

16. McDonnell, M. J. and Bates, R. H. T., "Restoring Parts of Scenes from Blurred Photographs", Opt. Commun., Vol. 13, pp. 347-349, March 1975.

17. Boulter, J. F., "Use of Two-Dimensional Digital Fourier Transforms for Image Processing and Analysis", DREV R-4025/75, July 1975, UNCLASSIFIED.

18. Bordua, J.-M., "Reconstitution d'images défocalisées et détériorées par un mouvement linéaire: une étude par simulation", CRDV M-2415/76, octobre 1976, NON CLASSIFIE.

19. Frieden, B. R., "Restoring with Maximum Likelihood and Maximum Entropy", J. Opt. Soc. Am., Vol. 62, pp. 511-518.

20. Frieden, B. R. and Swindell, W., "Restored Pictures of Ganymede, Moon of Jupiter", Science, Vol. 191, pp. 1237-1241, 26 March 1976.

21. Richardson, W. H., "Bayesian-Based Iterative Method of Image Restoration", J. Opt. Soc. Am., Vol. 62, pp. 55-59, January 1972.

22. Habibi, A., "Two Dimensional Bayesian Estimate of Images", Proc. IEEE, Vol. 60, pp. 878-883, July 1972.

23. Nahi, N. E. and Assefi, T., "Bayesian Recursive Image Estimation", IEEE Trans. Comp., Vol. C-21, pp. 734-738, July 1972.

24. Harris, J. L. Sr., "Image Evaluation and Restoration", J. Opt. Soc. Am., Vol. 56, pp. 569-574, May 1966.

25. McGlamery, B. L., "Restoration of Turbulence-Degraded Images", J. Opt. Soc. Am., Vol. 57, pp. 293-297, March 1967.

26. Andrews, H. C., "Computer Techniques in Image Processing", Academic Press, New York, 1970.

27. Arguello, R. J., Sellner, H. R. and Stuller, J. A., "Transfer Function Compensation of Sampled Imagery", IEEE Trans. Comp., Vol. C-21, pp. 812-818, July 1972.

28. Nahi, N. E., "Role of Recursive Estimation in Statistical Image Enhancement", Proc. IEEE, Vol. 60, pp. 872-877, July 1972.

29. Stockham, T. G., Jr., "Image Processing in the Context of a Visual Model", Proc. IEEE, Vol. 60, pp. 828-842, July 1972.

30. Lahart, M. J., "Maximum-Likelihood Restoration of Nonstationary Imagery", J. Opt. Soc. Am., Vol. 64, pp. 17-22, January 1974.

31. Huang, T. S., Barker, D. A. and Berger, S. P., "Iterative Image Restoration", Appl. Opt., Vol. 14, pp. 1165-1168, May 1975.

32. Huang, T. S. and Narendra, P. M., "Image Restoration by Singular Value Decomposition", Appl. Opt., Vol. 14, pp. 2213-2216, September 1975.

33. Huang, T. S., Burnett, J. W. and Deczky, A. G., "The Importance of Phase in Image Processing Filters", IEEE Trans. Acoustics, Speech and Signal Processing, Vol. ASSP-23, pp. 529-542, December 1975.

34. Stuller, J. A., "Linear Resolution Enhancement", Computer Graphics and Image Processing, Vol. 5, pp. 291-318, 1976.

35. Hawman, E. G., "Image Restoration Subject to Surface Area or Arc Length Constraints", J. Opt. Soc. Am., Vol. 67, pp. 76-81, January 1977.

36. Bergland, G. D., "A Guided Tour of the Fast Fourier Transform", IEEE Spectrum, pp. 41-52, July 1969.

37. "Selected Readings in Image Evaluation", Rodney Shaw, Editor, Waverly Press, USA, 1976.

38. Frieser, H., "Noise Spectrum of Developed Photographic Layers Exposed by Light, X-Rays, and Electrons", Photographic Science and Engineering, Vol. 3, pp. 164-169, July-August 1959.

39. DeBelder, M. and DeKerf, J., "The Determination of the Wiener Spectrum of Photographic Emulsion Layers with Digital Methods", Photographic Science and Engineering, Vol. 11, pp. 371-378, November-December 1967.

40. Billingsley, F. C., "Noise Considerations in Digital Image Processing Hardware", in Picture Processing and Digital Filtering, edited by T. S. Huang, Springer-Verlag, New York, 1975, pp. 249-281.

41. Zweig, H. J., Barrett, E. B. and Hu, P. C., "Noise-Cheating Image Enhancement", J. Opt. Soc. Am., Vol. 65, pp. 1347-1353, November 1975.

42. Higgins, G. C., "Methods for Analyzing the Photographic System, Including the Effects of Nonlinearity and Spatial Frequency Response", Photographic Science and Engineering, Vol. 15, pp. 106-118, March-April 1971.

43. Andrews, H. C., "Monochrome Digital Image Enhancement", Appl. Opt., Vol. 15, pp. 495-503, February 1976.

44. Gilchrist, A. W. R., "The Use and Properties of Window Functions in Spectrum Analysis", CRC R-1221, November 1971.

45. Boulter, J. F., "Use of Spatial Filtering to Match Wide Dynamic Range Grayscale Imagery to a Lower Resolution Display", DREV R-4074/77, January 1977, UNCLASSIFIED.

46. Sandor, T. and Cagliuso, G., "Rotating Drum Scanner-Display System for Digital Image Processing", Rev. Sci. Instrum., Vol. 45, pp. 506-509, April 1974.

47. Sévigny, L., "Programmathèque sur le traitement des images", CRDV R-4009/75, août 1975, NON CLASSIFIE.

CRDV R-4107/78 (UNCLASSIFIED)

Bureau - Recherche et Développement, Ministère de la Défense nationale, Canada.
CRDV, C.P. 880, Courcelette, Qué. G0A 1R0.

"Digital Restoration of Blurred Photographs"
by J.F. Boulter

La quantité d'information observable dans une photographie brouillée peut être augmentée si l'image est traitée dans un calculateur numérique. On décrit une procédure complète (qui est basée sur le filtrage de type Wiener) pour la reconstitution des photographies de haute résolution qui sont détériorées par plusieurs sortes de brouillage commun. On considère en détail les aspects pratiques d'une reconstitution acceptable. On décrit les limitations du filtre de Wiener, les caractéristiques du film photographique et des méthodes d'identification des brouillages par l'analyse des photographies brouillées. Des photographies de haute résolution défocalisées et détériorées par le mouvement qui est introduit directement dans la caméra sont reconstituées pour illustrer les techniques. (NC)

CRDV R-4107/78 (UNCLASSIFIED)

Bureau - Recherche et Développement, Ministère de la Défense nationale, Canada.
CRDV, C.P. 880, Courcelette, Qué. G0A 1R0.

"Digital Restoration of Blurred Photographs"
by J.F. Boulter

La quantité d'information observable dans une photographie brouillée peut être augmentée si l'image est traitée dans un calculateur numérique. On décrit une procédure complète (qui est basée sur le filtrage de type Wiener) pour la reconstitution des photographies de haute résolution qui sont détériorées par plusieurs sortes de brouillage commun. On considère en détail les aspects pratiques d'une reconstitution acceptable. On décrit les limitations du filtre de Wiener, les caractéristiques du film photographique et des méthodes d'identification des brouillages par l'analyse des photographies brouillées. Des photographies de haute résolution défocalisées et détériorées par le mouvement qui est introduit directement dans la caméra sont reconstituées pour illustrer les techniques. (NC)

CRDV R-4107/78 (UNCLASSIFIED)

Bureau - Recherche et Développement, Ministère de la Défense nationale, Canada.
CRDV, C.P. 880, Courcelette, Qué. G0A 1R0.

"Digital Restoration of Blurred Photographs"
by J.F. Boulter

La quantité d'information observable dans une photographie brouillée peut être augmentée si l'image est traitée dans un calculateur numérique. On décrit une procédure complète (qui est basée sur le filtrage de type Wiener) pour la reconstitution des photographies de haute résolution qui sont détériorées par plusieurs sortes de brouillage commun. On considère en détail les aspects pratiques d'une reconstitution acceptable. On décrit les limitations du filtre de Wiener, les caractéristiques du film photographique et des méthodes d'identification des brouillages par l'analyse des photographies brouillées. Des photographies de haute résolution défocalisées et détériorées par le mouvement qui est introduit directement dans la caméra sont reconstituées pour illustrer les techniques. (NC)

CRDV R-4107/78 (UNCLASSIFIED)

Bureau - Recherche et Développement, Ministère de la Défense nationale, Canada.
CRDV, C.P. 880, Courcelette, Qué. G0A 1R0.

"Digital Restoration of Blurred Photographs"
by J.F. Boulter

La quantité d'information observable dans une photographie brouillée peut être augmentée si l'image est traitée dans un calculateur numérique. On décrit une procédure complète (qui est basée sur le filtrage de type Wiener) pour la reconstitution des photographies de haute résolution qui sont détériorées par plusieurs sortes de brouillage commun. On considère en détail les aspects pratiques d'une reconstitution acceptable. On décrit les limitations du filtre de Wiener, les caractéristiques du film photographique et des méthodes d'identification des brouillages par l'analyse des photographies brouillées. Des photographies de haute résolution défocalisées et détériorées par le mouvement qui est introduit directement dans la caméra sont reconstituées pour illustrer les techniques. (NC)

DREV R-4107/78 (UNCLASSIFIED)

Research and Development Branch, Department of National Defence, Canada.
DREV, P.O. Box 880, Courcelette, Que. G0A 1R0.

"Digital Restoration of Blurred Photographs"
by J.F. Boulter

The amount of information that a human observer can obtain from a blurred photograph can be increased by post-processing the image in a digital computer. A complete procedure for restoring (by Wiener filtering) high-resolution photographs degraded by several common types of blurs is described. The practical aspects of obtaining an acceptable restoration are considered in detail. These include the limitations of the Wiener filter, the characteristics of photographic film and methods to identify the blur by analysing the blurred image using only limited a priori knowledge. High-resolution photographs degraded by motion and focus blurs introduced directly in a camera are restored to illustrate the techniques. (U)

DREV R-4107/78 (UNCLASSIFIED)

Research and Development Branch, Department of National Defence, Canada.
DREV, P.O. Box 880, Courcelette, Que. G0A 1R0.

"Digital Restoration of Blurred Photographs"
by J.F. Boulter

The amount of information that a human observer can obtain from a blurred photograph can be increased by post-processing the image in a digital computer. A complete procedure for restoring (by Wiener filtering) high-resolution photographs degraded by several common types of blurs is described. The practical aspects of obtaining an acceptable restoration are considered in detail. These include the limitations of the Wiener filter, the characteristics of photographic film and methods to identify the blur by analysing the blurred image using only limited a priori knowledge. High-resolution photographs degraded by motion and focus blurs introduced directly in a camera are restored to illustrate the techniques. (U)

DREV R-4107/78 (UNCLASSIFIED)

Research and Development Branch, Department of National Defence, Canada.
DREV, P.O. Box 880, Courcelette, Que. G0A 1R0.

"Digital Restoration of Blurred Photographs"
by J.F. Boulter

The amount of information that a human observer can obtain from a blurred photograph can be increased by post-processing the image in a digital computer. A complete procedure for restoring (by Wiener filtering) high-resolution photographs degraded by several common types of blurs is described. The practical aspects of obtaining an acceptable restoration are considered in detail. These include the limitations of the Wiener filter, the characteristics of photographic film and methods to identify the blur by analysing the blurred image using only limited a priori knowledge. High-resolution photographs degraded by motion and focus blurs introduced directly in a camera are restored to illustrate the techniques. (U)

DREV R-4107/78 (UNCLASSIFIED)

Research and Development Branch, Department of National Defence, Canada.
DREV, P.O. Box 880, Courcelette, Que. G0A 1R0.

"Digital Restoration of Blurred Photographs"
by J.F. Boulter

The amount of information that a human observer can obtain from a blurred photograph can be increased by post-processing the image in a digital computer. A complete procedure for restoring (by Wiener filtering) high-resolution photographs degraded by several common types of blurs is described. The practical aspects of obtaining an acceptable restoration are considered in detail. These include the limitations of the Wiener filter, the characteristics of photographic film and methods to identify the blur by analysing the blurred image using only limited a priori knowledge. High-resolution photographs degraded by motion and focus blurs introduced directly in a camera are restored to illustrate the techniques. (U)